

## Article

# Data Analytics Techniques for Performance Prediction of Steamflooding in Naturally Fractured Carbonate Reservoirs

Ali Shafiei <sup>1,\*</sup> , Mohammad Ali Ahmadi <sup>2</sup> , Maurice B. Dusseault <sup>3</sup>, Ali Elkamel <sup>4,5</sup>,  
Sohrab Zendehboudi <sup>2</sup>  and Ioannis Chatzis <sup>4,6</sup>

<sup>1</sup> Department of Petroleum Engineering, Schools of Mining and Geosciences, Nazarbayev University, Astana 010000, Kazakhstan

<sup>2</sup> Faculty of Engineering & Applied Science, Memorial University, St. John's, NL A1B3X7, Canada; m.a.ahmadi@mun.ca (M.A.A.); szendeboudi@mun.ca (S.Z.)

<sup>3</sup> Department of Earth and Environmental Sciences, University of Waterloo, Waterloo, ON N2L 3G2, Canada; mauriced@uwaterloo.ca

<sup>4</sup> Department of Chemical Engineering, University of Waterloo, Waterloo, ON N2L 3G2, Canada; aelkamel@uwaterloo.ca

<sup>5</sup> Department of Chemical Engineering, The Petroleum Institute, Khalifa University, Abu Dhabi 51900, UAE

<sup>6</sup> Department of Petroleum Engineering, College of Engineering and Petroleum, Kuwait University, Kuwait City 10002, Kuwait; ichatzis@uwaterloo.ca

\* Correspondence: ali.shafiei@nu.edu.kz or geomekker@gmail.com; Tel.: +7(717)269-4992

Received: 7 December 2017; Accepted: 19 January 2018; Published: 26 January 2018

**Abstract:** Thermal oil recovery techniques, including steam processes, account for more than 80% of the current global heavy oil, extra heavy oil, and bitumen production. Evaluation of Naturally Fractured Carbonate Reservoirs (NFCRs) for thermal heavy oil recovery using field pilot tests and exhaustive numerical and analytical modeling is expensive, complex, and personnel-intensive. Robust statistical models have not yet been proposed to predict cumulative steam to oil ratio (CSOR) and recovery factor (RF) during steamflooding in NFCRs as strong process performance indicators. In this paper, new statistical based techniques were developed using multivariable regression analysis for quick estimation of CSOR and RF in NFCRs subjected to steamflooding. The proposed data based models include vital parameters such as in situ fluid and reservoir properties. The data used are taken from experimental studies and rare field trials of vertical well steamflooding pilots in heavy oil NFCRs reported in the literature. The models show an average error of <6% for the worst cases and contain fewer empirical constants compared with existing correlations developed originally for oil sands. The interactions between the parameters were considered indicating that the initial oil saturation and oil viscosity are the most important predictive factors. The proposed models were successfully predicted CSOR and RF for two heavy oil NFCRs. Results of this study can be used for feasibility assessment of steamflooding in NFCRs.

**Keywords:** heavy oil; fractured carbonate reservoirs; steamflooding; cumulative steam to oil ratio; recovery factor; statistical predictive tools, digitalization, data analytics

## 1. Introduction

Consumption of liquid fuels, from both conventional and unconventional resources, will continue to be the primary source of energy in the decades to come. According to the International Energy Agency (IEA) in their World Energy Outlook 2015 report and some other reports from the U.S. Energy Information Administration (EIA) [1–3], global demand for oil is expected to grow from  $85.7 \times 10^6$  b/d [ $13.6 \times 10^6$  m<sup>3</sup>] in 2008 to  $103 \times 10^6$  b/d [ $16.37 \times 10^6$  m<sup>3</sup>] in 2030. The current global daily production

rate is now  $96.5 \times 10^6$  b/d. This is mostly due to expected world population growth combined with increasing per capita demand in growing economies such as China and India. As the dominant trend, much of the demand for liquid fuels comes from the transportation sector, which is expected to grow at about 1.4% each year until 2035. To meet the demand for liquid fuels in 2030, additional production of  $6.5 \times 10^6$  b/d [ $1 \times 10^6$  m<sup>3</sup>] will be needed. This is just a modest forecast as a reference scenario from the IEA and depending to the world economic conditions and other factors affecting the oil price and fuel consumption rate this figure is subject to change. The actual demand for oil could clearly be higher [1–3].

On the other hand, the sedimentary basins, especially the giant mostly carbonate fields in the Middle East, are drying fast and running out of cheap conventional oil with relatively easy production technology and in large volumes with the decline rates being on the range of 6–8% per year [4]. Obviously, there will be a growing gap between production and consumption. In the past decade, part of the gap was filled with contributions from unconventional resources. In this scenario, fossil petroleum liquids extracted from unconventional sources such as heavy oil, extra heavy oil, and bitumen will play a larger role in the decades ahead, as well. Development of non-conventional energy resources such as shale gas, shale oil and viscous oil (VO—including heavy oil, extra heavy oil, and bitumen) will fill part of the growing gap arising from a future decline in conventional oil production and the steady growth in demand for oil. However, due to large capital requirements and their relatively slow nature of development combined with technological, human capital, and economic challenges, a major and fast boost in their contribution to the global daily oil production is highly unlikely. Based on some EIA and IEA report, VO will comprise around 17% of the world daily oil production by 2035 and this also includes VO from NFCRs [1–3]. The current share of the VO to daily global oil production is about  $8\text{--}10 \times 10^6$  b/d [ $1.27\text{--}1.59 \times 10^6$  m<sup>3</sup>/d]; roughly 10% of the total oil production, and this represents a doubling of VO production in about 25 years.

The temperature sensitivity of VO viscosity controls the flow rate in all thermal production processes. This makes the in situ oil viscosity a far more important in technical and economic assessment than API gravity. Definitions of heavy oils in the literature are inconsistent, but many including the authors recommend that heavy oils be specified as oils with viscosities  $>100$  cP and  $<10,000$  cP under reservoir conditions. “Bitumen” can be defined as oils having viscosity  $>10,000$  cP in situ [5]. In this paper, VO refers to all crude oils with  $\mu > 100$  cP in situ; Heavy Oil (HO) refers to crude oil with  $100 < \mu < 10,000$  cP in situ; Extra Heavy Oil (XHO) refers to crude oil with  $\mu < 10,000$  cP in situ but with  $\rho > 1.0$  g/cm<sup>3</sup>; and bitumen refers to crude oil with  $\mu > 10,000$  cP in situ. A list of the various definitions and terms can be found in Dusseault and Shafiei [5] and Shafiei [6].

Almost 100% of the VO production from NFCRs comes from cold production operations in Oman, Iran, Iraq, Kuwait, Saudi Arabia, Turkey, and Mexico [6–8]. The VO in most of these reservoirs is mobile under reservoir conditions. Productive VO NFCRs are characterized by low matrix permeability and high fracture permeability, giving high early production that declines rapidly, leading to RFs below 3–5% in most cases [7]. Large-scale, early oil flux takes place through the high permeability and low volume fracture system, whereas the matrix-fracture interaction mainly controls the recovery efficiency and maintenance of longer-term smaller-scale production levels. VO production from NFCRs is in its very early days and is presenting major technical and economic challenges to the oil industry. These reservoirs are not yet widely commercialized and progress remains necessary for them to contribute a notable part of the daily worldwide oil production in the decades to come.

Several researchers have investigated important aspects of steamflooding (e.g., production mechanisms, productivity, wettability effects, process properties, feasibility) in homogeneous and heterogeneous porous media through experimental works, analytical modeling, and numerical modeling/simulations [9–27]. Most articles focus on steamflooding in unfractured (single porosity) systems. The interactive flux between the matrix block and fractures, and the consequent impact on the performance of steamflooding, are not well addressed in the literature.

Recovery Factor (RF) and Cumulative Steam to Oil Ratio (CSOR) are two critical economic parameters when evaluating an asset or designing a steamflood; accurate determination of these key parameters is of paramount interest in predicting viability of the thermal operation. Empirical models or correlations have not been yet developed to estimate CSOR and RF for steamflooding in VO NFCRs. However, various models and correlations are reported for performance prediction and analysis of various steam injection processes for VO production from oil sands and other unconsolidated sandstone VO reservoirs [9–27]. Some smart models have also been developed and introduced to assess the performance of steamflooding in NFCRs [10]. Without modifications to account for the different production characteristics, such correlations or models cannot be used for VO NFCRs. Overall, it is wise to expect higher CSOR, lower RF, lower thermal efficiency, and lower ultimate profitability for VO NFCRs steam processes compared with typical oil sands or unconsolidated sandstone VO steam injection processes.

Herein, data based techniques in terms of multivariate regression are developed for rapid estimation of CSOR and RF in VO NFCRs during steamflooding based on experimental and real field data [28–52]. The relationships involve major parameters such as in situ fluid and reservoir properties, and process conditions (e.g., steam flow rate and quality). Previous modeling and experimental studies with the aid of a statistical methods were used to determine the key variables that most strongly affect the CSOR and RF in both homogeneous (i.e., no natural fractures such as oil sands) and fractured reservoirs experiencing steamflooding. The data used are mainly from field pilots and some experimental test runs of steaming VO NFCRs. Employing the required production history, the correlations were then examined by statistical analysis strategies such as ANOVA, residual plots, and correlation coefficient calculations. The correlations were also qualitatively compared with the exiting correlations reported for oil sands and unconsolidated sandstones.

## 2. Steamflooding

A quick look at EOR surveys published over the past two decades shows that steam processes, including steamflooding and other processes involving steam injection, is so far the single commercially successful viscosity reduction method. It has been widely successful and broadly used in VO sandstones. More than 70% of global VO production involves steaming, and it is expected that this dominance will continue [53–60]. It should be noted here that we define commercially successful thermal operations as projects with production of at least 10,000 barrels per day for a reasonably long time. At the moment, this is only the case in oil sands and there is no commercial VO NFCR thermal operation.

Commercial VO thermal operations began in 1952 with vertical well steamflooding (SF) or steam drive (SD) (Figure 1) and their variants, mainly in California and then Venezuela [61]. These were generally implemented in thicker zones ( $>10$  m), and almost always for VOs with  $\mu < 5000$  cP, since initial communication between the offset wells is easily achievable only in cases of sufficient mobility (usually,  $k/\mu$  is higher than  $0.1$  mD/cP). Continuous steam injection at the base of an interval leads to creation of a slowly advancing and rising steam zone; the heat lowers the viscosity while volumetric sweep processes ( $\Delta p$ ) mobilize the fluids, displacing them to the production well.

CSOR values  $< 3$  for SD, SF, and CSS might be attained in thicker, high quality reservoirs ( $k \cdot h/\mu$  values greater than  $\sim 0.25$  mD·m/cP); however RF is likely to be substantially lower than gravity dominated thermal methods because of reservoir heterogeneity and advective instabilities (e.g., fingering and override). Cyclic steam stimulation (CSS) and gravity methods should achieve substantially lower CSOR values for a similar RF.

Low matrix permeability ( $<100$  mD), relatively low porosity ( $<20\%$ ) compared with a typical Canadian oil sand, medium to densely fractured media and fracture permeability ranging from low to very high are the most common characteristics of VO NFCRs. These, along with depth, represent major constraints for steam technology implementation. As a rough estimate, the VO volume in one cubic meter of oil sand (28–32% porosity) is about twice that of the typical VO carbonate reservoirs

(10–20% porosity). Compared to VO sands, steam processes in NFCRs will necessarily evidence higher CSOR and lower ultimate RF values, less thermal efficiency, and thus be economically less attractive. Permeabilities on the order of mD are very low when compared with a typical Canadian oil sand. Matrix permeability in some Canadian oil sands reaches up to 4000 to 5000 mD in some cases and in some fractured carbonated containing light oil permeabilities of few thousands mD is common. Heavy oil NFCRs are a poor type of reservoirs as they contain less oil and have lower effective permeability compared with oil sands. For the same volume of rock, NFCRs contain half the amount of oil in oil sands.

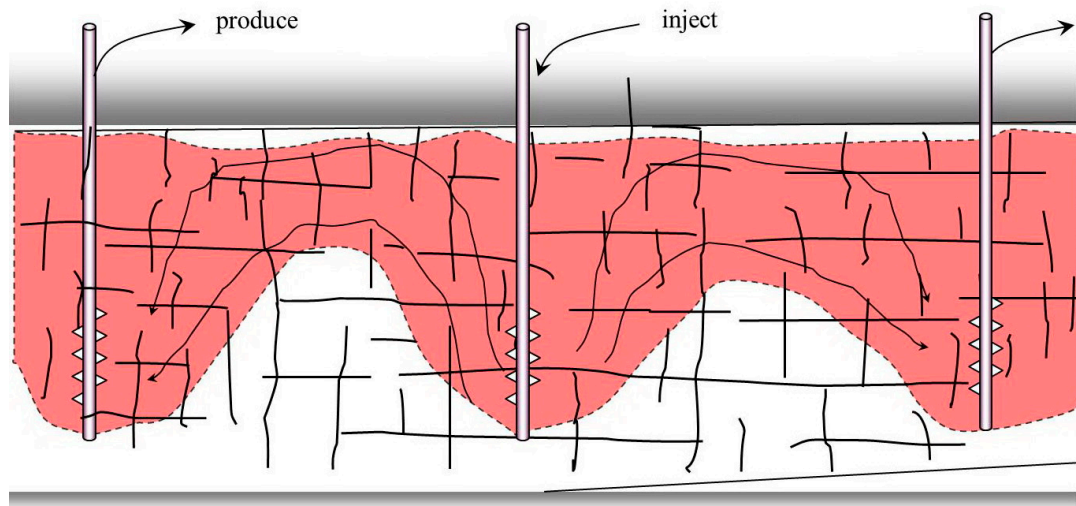


**Figure 1.** Steamflooding (SF) in NFCRs. This cartoon is a conceptual model of steamflooding in NFCRs taking into account the steamflooding experiences and the understanding we have from similar thermal operations in sandstones and oil sands and various effects such as steam override, and development of steam front. The black arrows show the flow direction and the red color shows the steam saturated zones or heated zones in the reservoir. The process involves continuous injection of steam typically with a row of injectors and the heavy oil that is mobile after heating up the reservoir and the heavy oil is displaced by steam toward production wells [10].

In several California fields (e.g., Kern River),  $RF > 70\%$  and  $CSOR = 4.35$  have been reported for steamflooding with very dense spacing (75–125 m) in a low tax and partly subsidized economic condition [62,63]. Using SF/SD techniques in highly favorable geological conditions (shallow, high  $k$ , and high initial oil saturation), high RF was achieved for Duri Field in Indonesia. However, a substantial heat losses, along with some steam breakthroughs to the surface and issues with steam override was reported [64,65]. Of course, all pressure-driven steam injection processes such as SF/SD and CSS experience advective and gravity instabilities (fingering, channeling, override) and therefore suffer from elevated heat losses. Hence, they are unlikely to be as efficient as gravity-dominated thermal extraction methods, where  $\Delta p \sim 0$  condition leads to diminution of all pressure-viscosity instabilities.

The screening criteria for SF/SD/CSS in oil sands and unconsolidated sandstones are presented in Table 1. One may refer to Dusseault and Shafiei [5], for a brief description and current status of application of steam technologies, and Boberg [66] and Butler [67] for production mechanisms involved in steam methods.

**Table 1.** Screening criteria for SF/SD/CSS in oil sands [68].

Parameter	Steaming Criteria	Comments
Minimum thickness	8–12 m (depending on net pay to gross pay—N/G—ratios)	Continuous net pay (N/G > 0.95) needed for thinner zones
Net pay	8–10 m—>0.95 15 m—can be 75–80% >15 m—<75% (high CSOR)	Shale is expensive to heat. CSS breaks through shales easier than SF/SD because of higher injection pressure
Shale beds	Beds < 2.5 m thick, lateral flow dominated process	CSS has more vertical flow requirement = better $k_v$ needed, comparatively
Porosity	20% (no known cases of commercial success at porosities less than 20%)	At low porosities, there is too much mineral matter to heat, in comparison to oil content
Permeability	>500–1000 mD	CSS more affected by intact barriers to vertical flow than SD/SF which require lateral flow capacity
Oil viscosity	<2000–5000 cP for SD/SF 5000 for CSS	SD/SF must have good well-to-well communication, not so for CSS
Steam pressure	<20 MPa, although in CSS, higher pressures may be needed for fracture injection	Depth-dependent, CSS in high $\mu$ oil uses fracture injection conditions but lower pressure during production than SD/SF
CSOR at $K \approx 1$ D (long term)	>10,000 cP > 3 to 4 >500 cP > 2	Dependent on reservoir quality and $\mu$ : higher $\mu$ = higher CSOR (slower process)
Recovery (RF)	40–70% (higher CSOR for high RF at the same viscosity)	RF strongly dependent on the full-cycle CSOR that the operator is willing to tolerate, but lower for higher viscosities
Active water	No CSS possible, SF/SD highly unlikely	Active water quenches steam (vacuum created) so significant barriers are needed

### 3. Production Mechanisms

Oil production from NFCRs using  $\Delta p$  processes generally occurs in two different stages: first, a pressure gradient within the fracture network acts as a driving force giving early (“flush”) oil production. Thereafter, oil is slowly displaced from within the matrix blocks by the pressure gradient from liquid and gas expansion, the pressure gradient enforced between wells, and aided somewhat by gravity drainage forces in the presence of a light (steam) phase. The oil slowly released and displaced from the matrix, flows via the fracture network to the production wells. Different driving mechanisms including solution gas liberation and expansion, distillation of steam, generation of carbon dioxide, capillary imbibition, and gravity drainage are active during continuous steaming of a VO NFCR [69]. The most effective recovery mechanism within the matrix blocks is thermally- and  $\Delta p$ -induced liquid and gas expansion, displacing the oil to the fractures. High temperatures reduce the oil viscosity, permitting these processes, including the fracture flow, to take place more quickly.

Hernandez and Trevisan proposed two numerical modeling/simulations to investigate heating process in rock matrix [69]. The first model describes the heating mechanism in a horizontal cross section of a matrix block surrounded by a fracture with steadily steam flow. The second model uses a vertical cross section to incorporate gravity effects due to phase density differences. These scientists concluded that steam distillation is the most effective oil recovery mechanism in NFRs. This is because the steam distillation allows full recovery of  $\text{CH}_4$  along with the light and medium components in the oil phase (these vaporize and therefore are highly mobile and more easily recoverable). Solution gas expansion ( $+\Delta T$ ,  $-\Delta p$ ) sustains the pressure difference between the matrix and the fracture and preferentially displaces the distilled phases. The high viscosity of the remnant oil, due to the liberation of light compounds, limits the contribution of capillary imbibition mechanisms to oil recovery from matrix.

The solution gases driven off and their expansion, as well as the liquid expansion, dominate the drive energy. Because the matrix block permeability in many NFCRs is less than 100 mD, gravity segregation within the blocks is slow to negligible, although very rapid in the vertical fracture network, maintaining high early  $\Delta p$  between fractures and matrix. Viscosity reduction is not an energy source in itself, although the associated temperature is the dominant agent in gaseous phase exsolution and



fluid expansion. Because the gas expansion tends to displace the oil and the gravity effects tend to cause the gas to rise, especially in the fractures, oil recovery is somewhat earlier, and gas production somewhat delayed.

Generation of carbon dioxide is responsible for amelioration in recovery of distilled components from the oil phase and for the recovery of liquid fractions. A complete discussion of these complex and interacting production mechanisms can be accessed elsewhere, such as [70–74].

#### 4. CSOR and RF Prediction

Cumulative Steam to Oil Ratio (CSOR) is the volume ratio of water injected as steam to oil produced at stock tank conditions. CSOR (or its inverse) is used to gauge steamflooding methods' economic success; it is the most common way of expressing thermal efficiency. Recovery Factor (RF) is the other important economic parameter, though not in the absence of CSOR. There are various equations available in the literature for performance forecast of a variety of steam processes in oil sands or unconsolidated sandstone VO reservoirs [44,66,67,75]. Chu [20] proposed the following empirical correlations based on statistical analysis of 28 successful SF/SD operations in oil sands to estimate the CSOR:

If  $CSOR \leq 5$  (Metric units)

$$CSOR = 18.744 + 0.004767D - 0.16693h - 0.8981K - 0.5915\mu - 14.79S_o - 0.0009767\frac{Kh}{\mu} \quad (1)$$

If  $CSOR \geq 5$  (Metric units)

$$CSOR = -0.011253 - 0.00009117D + 0.0005180h - 0.07775\varphi - 0.007232\mu + 0.00003467Kh/\mu + 0.5120S_o \quad (2)$$

In these correlative functions,  $D$  is the depth (m),  $h$  is the thickness (m),  $K$  is the permeability (mD),  $S_o$  is the oil saturation,  $T$  is the temperature in °C,  $\mu$  is the viscosity in Pa·s, and  $\varphi$  is the porosity as a bulk volume fraction. The advantage of using such correlations is that they are based on well-known reservoir parameters and do not required simulation or iterative calculations. Chu (1985) [44] recommended using a CSOR of 10 as the cut off for economic feasibility of any steaming operation; of course, this is highly dependent on the price of steam (generally from CH<sub>4</sub> combustion) and the price of oil.

Vogel [75] developed a model for steamflooding considering the steam over-ride effect (gravity segregation of gases and liquids). He also assumed that the injected steam overlays the formation immediately and then conducts heat upwards (vertically) to the overburden and downward into the reservoir. CSOR can be calculated using Vogel's model as follows [75]:

$$COSR = \frac{62.4h_s\varphi SH_t}{\Delta T[h_s(\rho c)_s + 2(K_{h1}\sqrt{t/\pi\alpha_1} + K_{h2}\sqrt{t/\pi\alpha_2})]} \quad (3)$$

where  $h_s$  is the thickness of steam zone (ft),  $(\rho c)_s$  is the steam zone volumetric heat capacity (Btu/ft<sup>3</sup>–°F),  $\Delta T = T_s - T_r$  (°F) is the difference between steam and initial reservoir temperature,  $\alpha_1$  and  $\alpha_2$  are the thermal diffusivity values of overburden and oil sand, respectively (ft<sup>2</sup>/h<sub>r</sub>),  $t$  is the time of steam injection (h<sub>r</sub>), and  $K_{h1}$  and  $K_{h2}$  are the thermal conductivity of overburden and oil sand layer, respectively (Btu/h<sub>r</sub>–ft–°F).  $\Delta S$  and  $H_t$  are defined as:

$$\Delta S = S_{oi} - S_{ors}, H_t = \overline{X}_l H_{WV} + H_{WS} - H_{Wr} \quad (4)$$

Here,  $S_{oi}$  is the initial oil saturation prior to steamflood (fraction),  $S_{ors}$  is the average steam zone oil saturation at breakthrough (fraction), and  $H_t$  is the total enthalpy energy injected (Btu/lb),  $H_{WV}$  is the latent heat of water vaporization at downhole injection pressure and temperature (Btu/lb),  $H_{WS}$  is

the enthalpy of liquid water at downhole injection pressure and temperature, Btu/lb, and  $H_{Wr}$  is the enthalpy of liquid water at original reservoir conditions, Btu/lb, and  $(\bar{X})$  is the average downhole steam quality during injection (lb/lb).

Boberg [66] proposed the following equation using Marx-Langenheim's model for estimation of CSOR during steamflooding based on thermal efficiency calculations:

$$\text{COSR} = \frac{62.4\phi h E_h [(\bar{X}_i H_{WV}(S_{oi} - S_{ors}))]}{B_o h_t (T_s - T_r)(\rho c)_{R+F}} \quad (5)$$

where  $T_s$  and  $T_r$  are the steam temperature and reservoir temperature ( $^{\circ}\text{F}$ ),  $B_o$  is the oil content of the reservoir,  $h_t$  is the reservoir net pay thickness (ft), and  $E_h$  is the thermal efficiency.

Butler [67] introduced the following relationship to predict CSOR of steamflooding in oil sands. He employed thermal efficiency computations for constant displacement rate steam drive, relating the cumulative displaced oil ( $\phi \Delta S_o h A$ ) to the cumulative injected heat into the reservoir:

$$\text{COSR} = \frac{H_s \phi (S_o - S_{or})}{\rho_1 C_1 (T_s - T_r)} \left( \frac{1}{1 + \frac{8}{3} \left( \frac{K_2}{\rho_1 C_1 h} \sqrt{t / \pi \alpha_2} \right)} \right) \quad (6)$$

Here,  $H_s$  is the enthalpy of steam (Btu/lb),  $\alpha$  is the thermal diffusivity ( $\text{ft}^2/\text{d}$ ), and  $\rho C$  is the volumetric heat capacity of the steamed reservoir ( $\text{Btu}/\text{ft}^3\text{-}^{\circ}\text{F}$ ).

## 5. Data Collection

A limited number of steamflooding pilots can be found in the literature. The pilot operations are tried in France, Italy, Congo, Turkey, USA, Kuwait, and Saudi Arabia [28–43]. The first part of the data collected and used in this study is from field pilots of steamflooding in VO NFCRs reported in the literature.

The important parameters for SF field tests are summarized in Table 2. To increase the size of the database, some data from pilot plants executed in highly fractured light oil NFCR's and viscous oil highly fractured sandstone reservoirs were included [35,42,44]. In addition, some experimental data were taken from studies conducted on steamflooding in fractured media available in the literature [45–52]. The data available covers a range of fluid and reservoir properties under different operational conditions.

**Table 2.** Characteristics of the steamflooding field pilots conducted in NFRCs.

Field	Lacq Superieur, SW France	Ikiztepe, SE Turkey	Emeraude, Offshore Congo on the West African Coast		Yates Field, Permian Basin of West Texas
Reservoir	Lacq Superieur	Ikiztepe	R1	R2	San Andres dolomite
Geology	Heterogeneous and fractured calcareous or dolomitic formations	The Sinan vuggy and fractured limestone	A succession of siltstones and highly fractured low matrix permeability limestones		Fractured dolomite
OOIP ( $1 \times 10^6$ b)	125	127	5000		n/a
Depth (m)	600–700	1350	186–249	249–297	457
Thickness (m)	120	100–150	50	48	n/a
$\mu$ (cP)	17 (Medium heavy oil)	936 (Heavy oil)	100		6
$P_{ro}$ (MPa)	6	12.7	3.1		n/a
$T_{ro}$ ( $^{\circ}$ C)	60	49	31		27
$\varphi_m$ (Fraction)	0.12	0.15–0.30	0.2–0.3		0.15–0.17
$K_m$ (mD)	1	50–400	0.1–50	>50	100–170
$K_f$ (mD)	5000–10,000	1000	>1000		>1000
Formation volume factor	1.04	1.056	1.01		n/a
Steam quality (%)	80	60–80	80		80
CSOR	5.5	3.1	1.45	3.98	8.8
Cumulative steam injected (MCWEB)	970	81	480	700	910
Cumulative oil production (b)	176	26	315	176	103
Field	Wafra, Neutral Zone (Saudi Arabia and Kuwait)		Naval Petroleum Reserve No. 3 (NPR-3), Teapot Dome Field, Wyoming		
Reservoir	2nd Eocene		1B-South	1C-East	3A 4A
Geology	Dolomite		The Shannon, composed of the Upper and Lower Shannon sandstones		
OOIP ( $1 \times 10^6$ b)	7000		0.748	0.748	1.48 1.46
Depth (m)	580–670		134–146	134–146	134–146 134–146
Thickness (m)	n/a		7–14	7–14	7–14 7–14
$\mu$ (cP)	30–250		10	10	10 10
$P_{ro}$ (MPa)	n/a		2.34	2.34	2.34 2.34
$T_{ro}$ ( $^{\circ}$ C)	n/a		18	18	18 18
$\varphi_m$ (Fraction)	n/a		0.16–0.2	0.16–0.2	0.16–0.2 0.16–0.2
$K_m$ (mD)	n/a		18–65	18–65	18–65 18–65
CSOR	5.55		9.42	9.5	13.38 10.9
Cumulative steam injected (MCWEB) *	1000		2011	1693	3679 1302
Cumulative oil production ( $1 \times 10^3$ b)	180		213	176	133.7 119

\* MCWEB = 1000 Cold Water Equivalent Barrels.



## 6. Methodology

Different experimental and numerical models were studied to understand the main parameters, their interactions, and trends during steamflooding process. The earlier correlations developed for prediction of CSOR in oil sands, for instance Chu [20] did not take into account all the major parameters and their interrelationships during steamflooding. The most important variables for statistical analysis were determined to be in situ viscosity, effective porosity, fracture permeability, matrix permeability, reservoir thickness, depth, steam flow rate, steam quality, and initial oil saturation.

Reliable field data and well-documented field trials are the foundation of developing statistical screening tools. However, a limited number of successful case histories (partially or marginally so in some cases) or field trials exist for steamflooding in VO NFCRs. All the field pilots of steamflooding in VO NFCRs available in the literature were studied to assemble a database, and as many of the critical parameters as we could were collected or calculated for this study (see Shafiei et al. [10] for the database). To enhance the value of statistical analysis, the database was extended to include steamflooding trials in highly (naturally) fractured sandstone viscous oil reservoirs, and some experimental data from similar cases was incorporated as well. We tried to make sure that all the data collected and used in this study are fully compatible with the physics of vertical well steamflooding in naturally fractured media.

To examine results of multiple linear regression analysis and determine the dependency of a given response variable on a special fluid or/and reservoir property, scatter plots are usually generated [76,77]. These plots can show the absolute effect of each independent variable on the response variables. This statistical analysis first assumes no interactions among the identified predictor variables (e.g., no interaction terms). In this case, the correlation equation would have the following form for “ $k$ ” regressor variables:

$$y = \beta_0 + \beta_1 x_1 + \beta_2 x_2 + \dots + \beta_k x_k + e \quad (7)$$

The parameters “ $\beta_0$  to  $\beta_k$ ” are the regression coefficients;  $x_1, x_2, \dots, x_k$  are the independent variables, also known as dimensionless numbers; and “ $y$ ” is the actual response variable. Some interaction terms also can be introduced to forecast the behavior of the reservoir during steam injection. The model connecting the regressor to the response,  $y_i$ , is as the following:

$$y_i = \beta_0 + \beta_1 x_{i1} + \beta_2 x_{i2} + \dots + \beta_k x_{ik} + e_i \quad i = 1, 2, \dots, n \quad (8)$$

For “ $n$ ” number of observations (field data or/and experimental measurements), this represents a system of “ $n$ ” equations which can be expressed in the matrix notation as the following:

$$y = X\beta + e \quad (9)$$

where:

$$y = \begin{bmatrix} y_1 \\ y_2 \\ \vdots \\ y_n \end{bmatrix}, X = \begin{bmatrix} 1 & x_{11} & x_{12} & \cdots & x_{1k} \\ 1 & x_{21} & x_{22} & \cdots & x_{2k} \\ \vdots & \vdots & \vdots & & \vdots \\ 1 & x_{n1} & x_{n2} & \cdots & x_{nk} \end{bmatrix}, \beta = \begin{bmatrix} \beta_0 \\ \beta_1 \\ \vdots \\ \beta_k \end{bmatrix}, \text{ and } e = \begin{bmatrix} e_1 \\ e_2 \\ \vdots \\ e_n \end{bmatrix} \quad (10)$$

The least square estimate of “ $\beta$ ” can be calculated as the following:

$$\hat{\beta} = (X'X)^{-1}X'y \quad (11)$$

The physics of steamflooding in VO NFCRs suggests that a set of dependent dimensionless control the magnitudes of the objective functions. Hence, regression models should accommodate the so-called “effect of interaction between the dependent terms”. Interaction between two dependent variables can be defined as a cross product term in the model:

$$y = \beta_0 + \beta_1 x_1 + \beta_2 x_2 + \beta_{12} x_1 x_2 + e \quad (12)$$

After the required parameters such as CSOR were collected from the pilot plant and laboratory studies, they were substituted in the corresponding equations to conduct a parametric sensitivity analysis to determine the proper relationships between the target function and key independent variable. The procedure to obtain scatter plots and the predictive equation for CSOR is given briefly as follows:

A systematic parametric sensitivity analysis should be conducted through the following steps to determine the proper relationships between the target function (s) and key independent variables:

- The CSOR values are obtained from the data;
- CSOR is plotted separately versus all key parameters with other variables kept constant;
- When all figures for CSOR are plotted, a general correlation for CSOR versus dependent variables with unknown coefficients of contributing terms can be obtained; and,
- Using Equations (7) through (10), regression coefficients are calculated (for this we used MATLAB™ and Excel™).
- This approach is also used for the other major economic assessment metric—recovery factor (RF).

Three main validity measures are employed when examining the suitability of multivariate linear regression analysis: residual analysis, ANOVA tables, and analysis of square of residuals:

Data from a standard sum of squares of the variance analysis are included in the ANOVA table. The ANOVA table contains the data for each of two deviation sources. This includes both the regression and the residuals (e.g., 1st column in Tables 3 and 4). The total deviation is defined as the sum of regression and residuals. The source of variation is due to deviation of each forecasted data point either from its group mean value (e.g., regression) or from its observed value (i.e., residuals). The sum of these two sources of variance comprises the total variance. Four variance measures (e.g., columns 3–5 in Tables 3 and 4) are introduced for each of the deviations sources as the following:

- Degrees of freedom (e.g., DF, 2nd column of Tables 3 and 4): DF can be defined as the number of correlation coefficients (N) for each special regression analysis with respect to the number of regressor variables implemented in the model.
- Sum of the Squares (e.g., SS; 3rd column of Tables 3 and 4): SS can be calculated using the observed data and the predicted results. SS is a measure of variance for each special regression analysis. The total SS can be calculated via summation of the squares of the residuals plus the sum of the squares of regression:

$$\sum_{i=1}^n (y_i - \bar{y})^2 = \sum_{i=1}^n (\hat{y}_i - \bar{y})^2 + \sum_{i=1}^n (y_i - \hat{y}_i)^2 \quad (13)$$

where  $y_i$  and  $\hat{y}_i$  are real (or observed) data and predicted data, respectively.  $n$  is the number of observations (data points).  $\bar{y}$  refers to the average of all data points of dependent variable expressed by the following equation:

$$\bar{y} = \frac{\sum_{i=1}^n y_i}{n} \quad (14)$$

- Mean squares (e.g., MS; 4th column of Tables 3 and 4). MS is the sum of squares adjusted for the DF (Degree of Freedom).
- F test (e.g., F; 5th column of Tables 3 and 4): F is a statistical parameter related to variance, which compares two models with different regressor variables. The goal here is to check whether the more complex model is a better predictor or not. Normally, if the F is bigger than a standard tabulated value then the more complex equation is considered superior [76,77]. The significance level is usually set at 0.05.

**Table 3.** Regression model of the CSOR ( $R^2 = 0.96$ ;  $F = 196.6$ ).

Coefficient	Numeric Value	Standard Error	Lower 95%	Upper 95%
a0	−15.5	2.85	−29.65	−5.0500
a1	−0.001	0.0003	−0.0018	−0.0002
a2	6.87	1.85	2.98	10.76
a3	4151.45	283.52	404	7898
a4	0.000005	0.0000001	0.000002	0.000008
a5	−221.21	18.59	−260	−182
a6	22.49	3.73	14.65	30.34
a7	−46,579	4306	−55,626	−37,532
a8	−2.54	0.11	−4.67	−0.97
a9	−7.14	1.17	−9.60	−4.68
a10	0.031	0.009	0.01	0.05
a11	151,755	14,188	121,947	181,563
a12	18,116	1349	15,282	20,950
a13	−1289	146.7	−2081	−498
a14	0.0053	0.0002	0.0008	0.009

**Table 4.** Information for the Linear Regression Model of the RF prediction ( $R^2 = 0.964$ ;  $F = 79.317$ ).

Coefficients	Numeric Value	Standard Error	Lower 95%	Upper 95%
a15	−85.8	26.52	−140.15	−31.50
a16	137.5	30.24	46.82	228.19
a17	0.02	0.01	0.0007	0.04
a18	0.21	0.04	0.12	0.31
a19	282.3	41.53	111.48	453.1
a20	−0.0009	0.0002	−0.001	−0.0004
a21	47	7.07	26.36	67.64
a22	−0.0003	0.0001	−0.0005	−0.00008
a23	−0.03	0.02	−0.07	0.015
a24	−213.1	80.3	−505.3	−2.89
a25	−0.16	0.03	−0.22	−0.09
a26	0.0006	0.0002	0.0002	0.12
a27	−0.49	0.01	−0.78	−0.20
a28	−0.01	0.003	−0.06	−0.007

## 7. Results and Discussion

Predictive tools for screening viscous oil reservoirs for a certain production technology can be valuable instruments when assessing technical feasibility and the potential performance of the process in a candidate reservoir. Two quick predictive models were developed here to estimate RF and CSOR in NFCRs that undergo steamflooding for heavy oil recovery. It is important to note that the steamflooding operation is generally ended when the cumulative steam oil ratio (CSOR) reaches the value of 60. Thus, the performance of steamflooding process is evaluated at this cut-off point.

### 7.1. Regression Analysis

Scatter plots (Figures 2–11 for CSOR and Figures 12–21 for RF) show the dependency of a special response variable on a special fluid or/and reservoir property. Figures 2–7 and Figures 12–17 are obtained for the physical models with the same pattern (in shape and number of fractures) and the same dimensions in most cases. In addition, it is clear that all properties for steamflooding processes demonstrated on each figure except those on  $x$  and  $y$ -axes are the same when investigating effect of an independent variable on target functions. This conveys the message that these figures just present a limited volume of data used in this study to point out the important trends in performance of reservoirs during steamflooding according to a comprehensive parametric sensitivity analysis. Based on Figures 2–7, CSOR increases with an increase in oil viscosity, steam injection rate, fracture to matrix permeability, and gross to net reservoir thickness. However, high steam quality and high initial oil saturation lead to reductions in CSOR, indicating better response to steam injection. In addition,

Figures 2–11 for CSOR indicate acceptable agreement between the field data and the predictions. It is clear that increase in steam injection rate improves the recovery rate but lowers the RF before steam breakthrough in fractured media (particularly highly fractured ones), as presented in Figure 12. Furthermore, if the reservoir contains oil with high viscosity, some areas can be bypassed during steamflooding, resulting in early breakthrough and consequently lower RF, as demonstrated in Figure 13. The same effect may occur when there are many fractures with high permeability in the reservoir (see Figure 14). Although the presence of fractures can cause an increase in the rate of oil production, a high density of fractures may have undesired effects on the overall performance of steamflooding, as depicted in Figure 14. Figure 15 shows that the ratio of the reservoir depth to the reservoir thickness does not have a noticeable impact on RF during steamflooding. As expected, steam quality and initial oil saturation have direct impacts on magnitude of RF. Increase in these two parameters can improve the performance of the steamflood (see Figures 16 and 17). Clearly, steam injection with higher quality steam enters more heat into the reservoir leading to an increase in temperature. Hence, it causes viscosity reduction that enhances the oil recovery. The figures related to RF again confirm the effectiveness of the statistical approach adopted in this study as a good match was observed between the field data and the results obtained from the correlations.

Figures 10 and 11 are the residual plots for the CSOR with respect to porosity and a combined interaction component (including formation depth and thickness), respectively. In addition, residual plots for RF versus porosity and “steam quality multiplied by steam injection rate” are presented in Figures 20 and 21, respectively, as two samples of the analysis of the residuals. For these four residual plots, the residual data shows random distribution all along the horizontal axis. In other words, the proposed linear regressions are valid for CSOR and RF in terms of the particular dependent variables shown on  $x$ -axis.

These results show that CSOR values for viscous oil extraction from NFCRs and some highly naturally fractured sandstone reservoirs can be correlated with reservoir and oil characteristics such as permeability, porosity, thickness, viscosity, and oil saturation. The following empirical relationship predictive function was developed in this study to estimate the CSOR during vertical well steamflooding in a NFCRs:

$$\text{CSOR} = a_0 + a_1 D + a_2 \frac{1}{\varphi_e} + a_3 \frac{1}{K_m} + a_4 K_f + a_5 \frac{1}{\mu_o} + a_6 \frac{1}{S_o} + a_7 \frac{1}{q_s} + a_8 x_s + a_9 \frac{1}{S_o \varphi_e} + a_{10} \frac{D}{h} + a_{11} \frac{D}{h \varphi_e K_m \mu_o S_o q_s} + a_{12} \frac{1}{\varphi_e q_s} + a_{13} \frac{1}{\varphi_e K_m} + a_{14} \frac{K_f}{K_m} \quad (15)$$

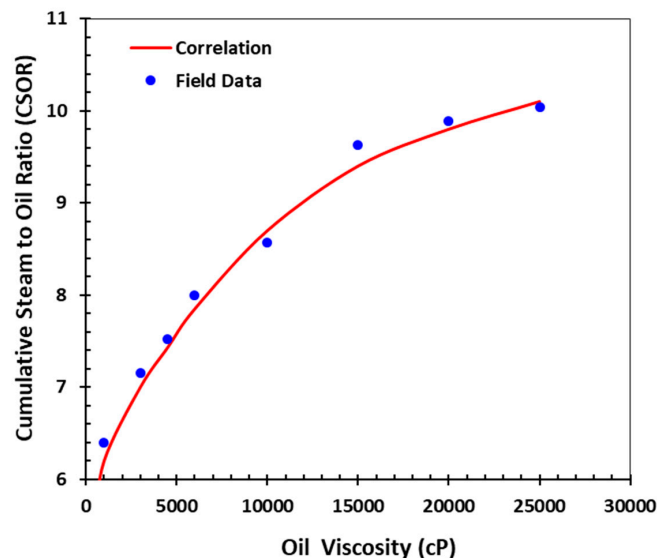


Figure 2. CSOR vs. oil viscosity for the database analyzed.

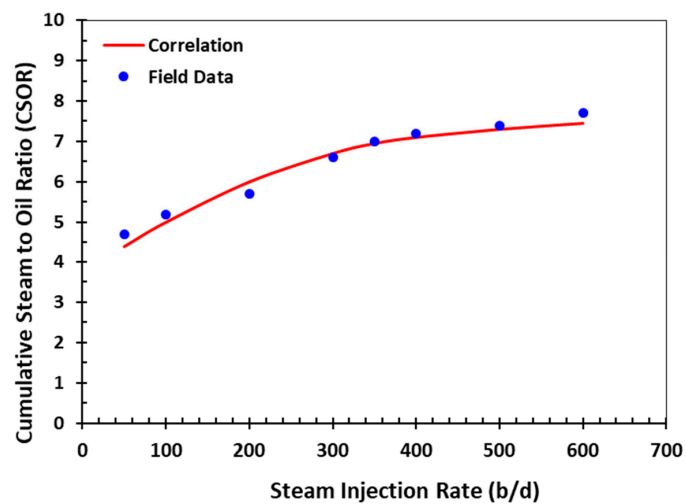


Figure 3. CSOR vs. steam injection rate for the database analyzed.

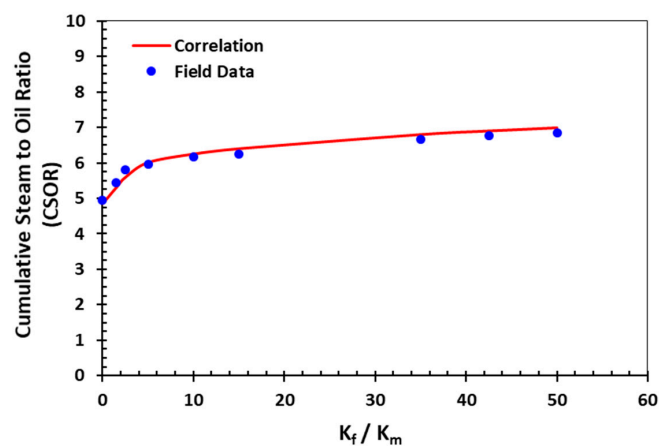


Figure 4. CSOR vs. fracture to matrix permeability ratio for the database analyzed.

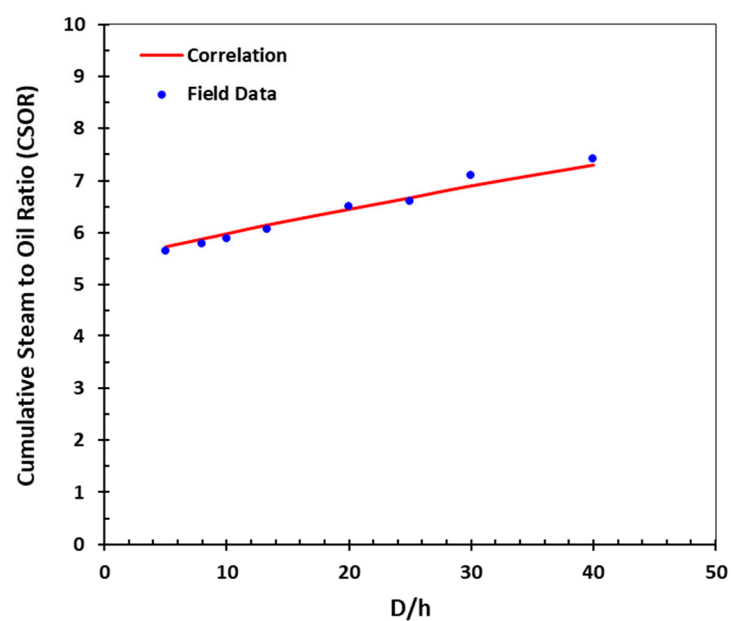


Figure 5. CSOR vs. gross to net thickness ratio for the database analyzed.

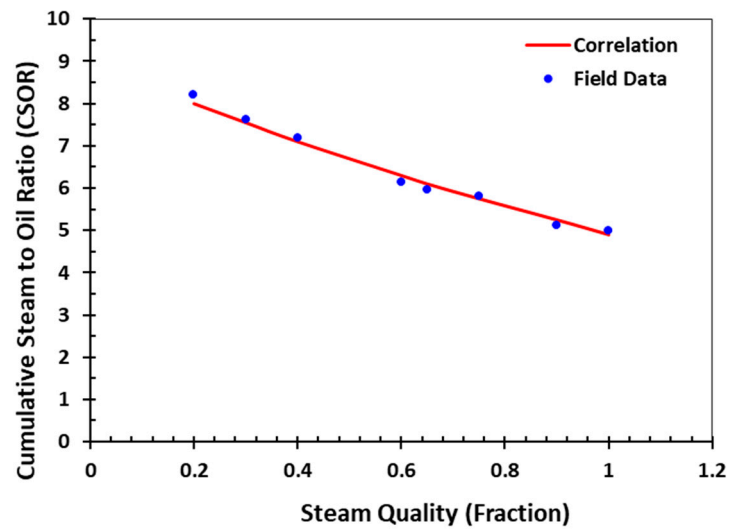


Figure 6. CSOR vs. steam quality for the database analyzed.

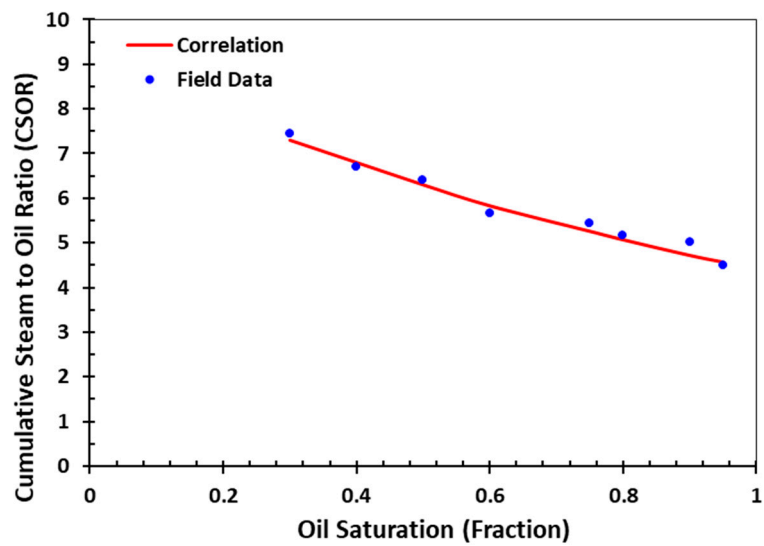


Figure 7. CSOR vs. oil saturation for the database analyzed.

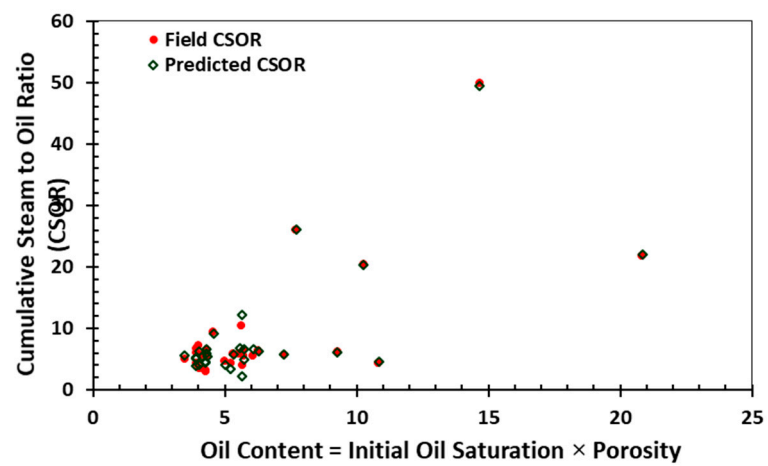


Figure 8. CSOR vs. oil content for the database analyzed.



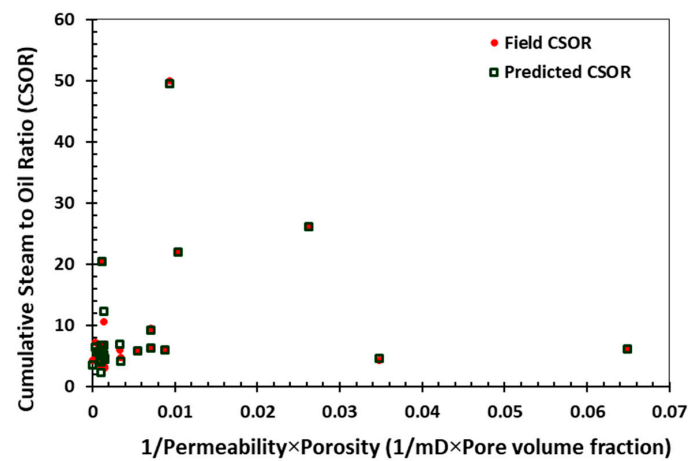


Figure 9. CSOR vs.  $1/K \times \phi$  for the database analyzed.

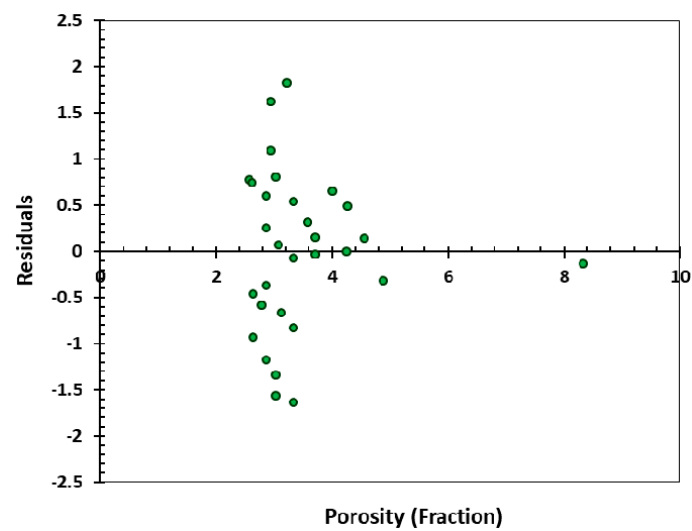


Figure 10. Residuals vs. porosity for the database analyzed.

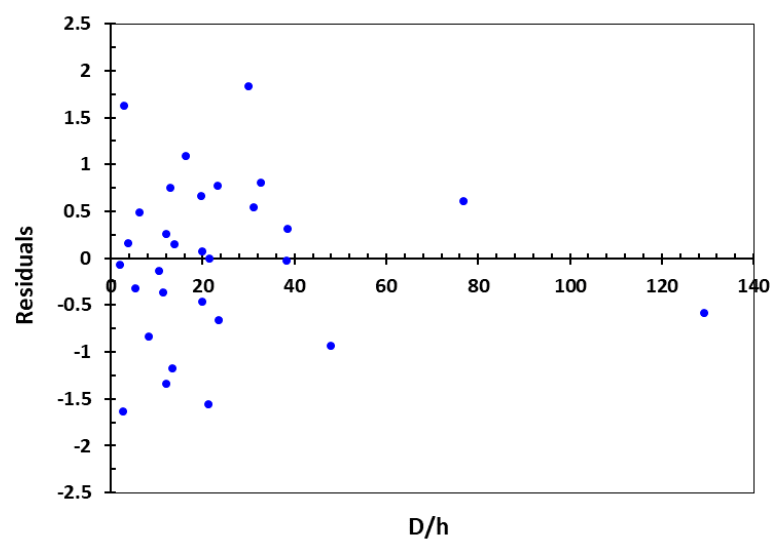


Figure 11. Residuals vs. gross to net thickness ratio for the database analyzed.

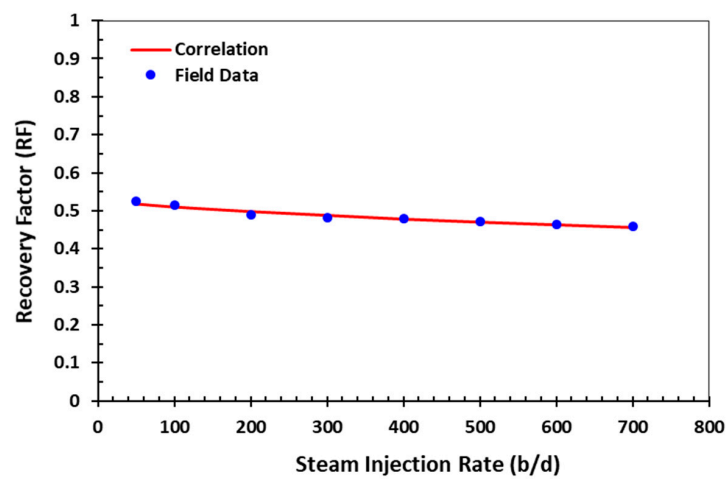


Figure 12. RF vs. steam flow rate for the database analyzed.

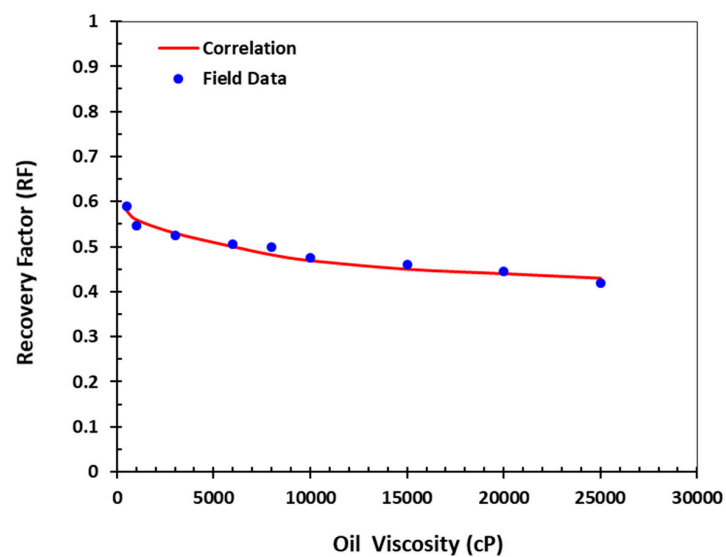


Figure 13. RF vs. oil viscosity for the database analyzed.

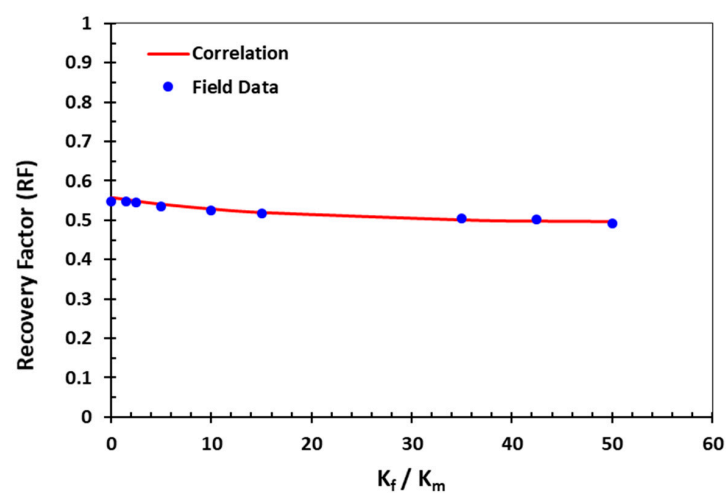


Figure 14. RF vs. fracture permeability to matrix permeability ratio for the database analyzed.

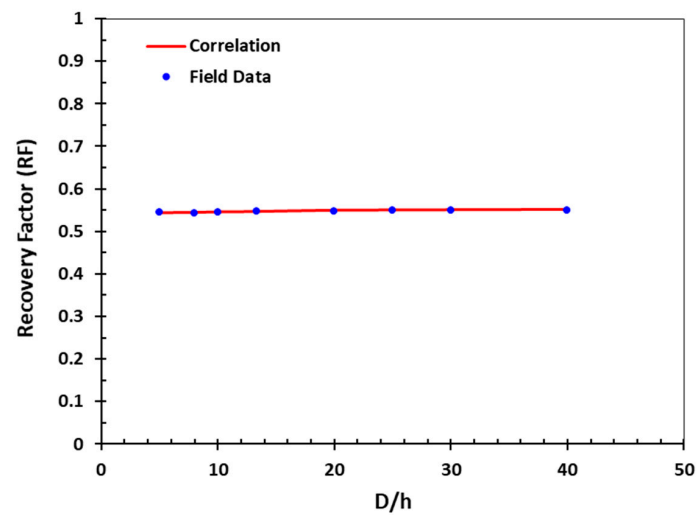


Figure 15. RF vs. gross to net thickness ratio for the database analyzed.

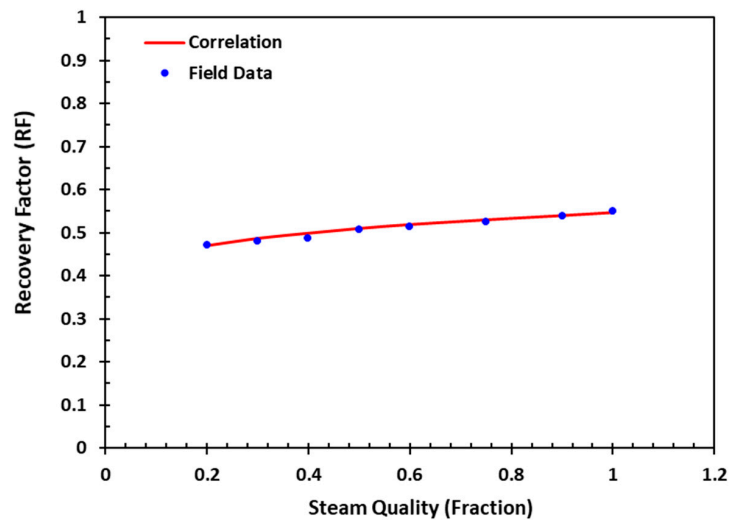


Figure 16. RF vs. steam quality for the database analyzed.

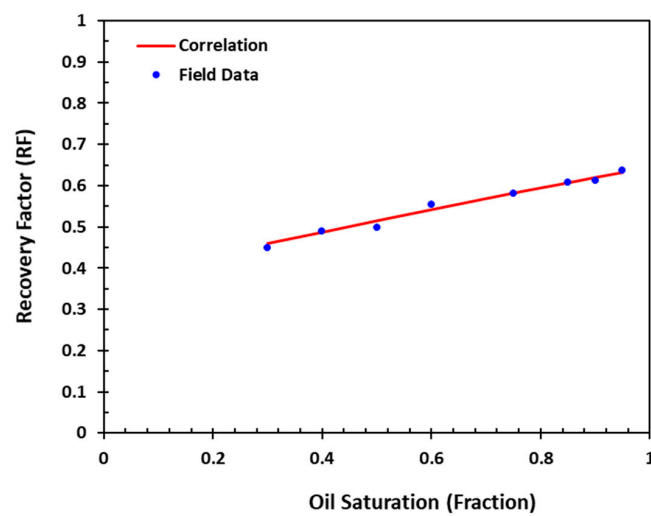


Figure 17. RF vs. oil saturation for the database analyzed.

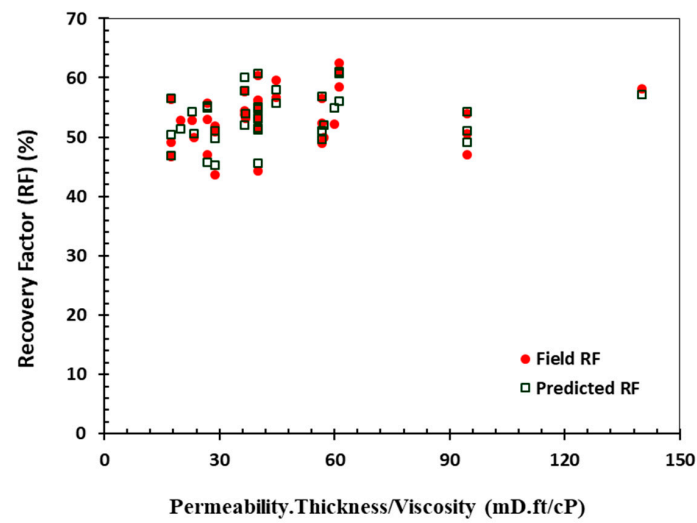


Figure 18. RF vs. producibility factor for the database analyzed.

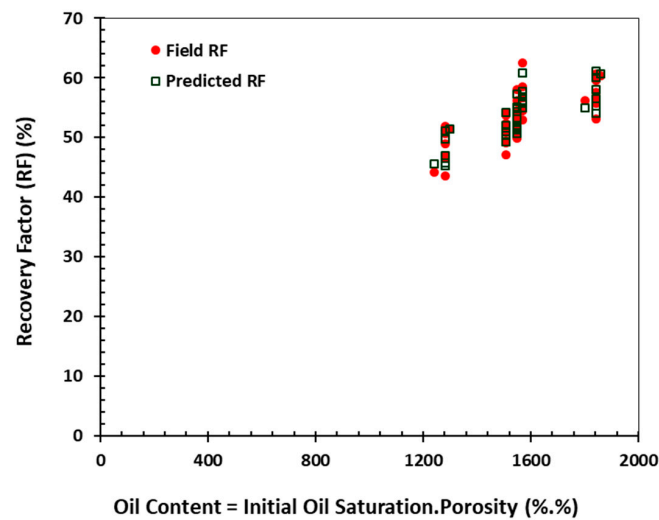


Figure 19. RF vs. oil content for the database analyzed.

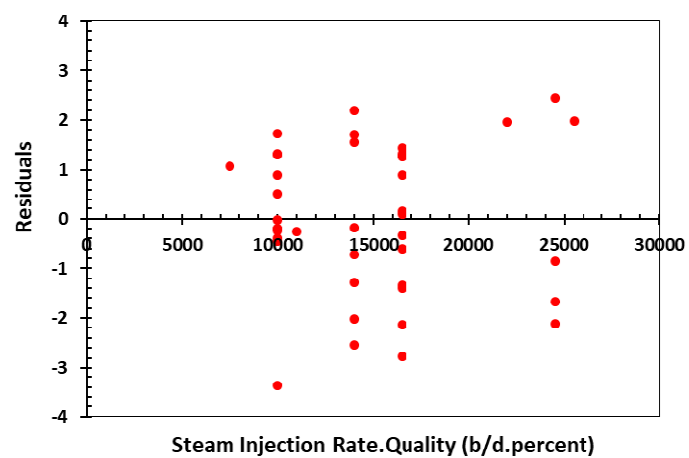


Figure 20. Residuals vs. product of steam injection rate and quality for the database analyzed.

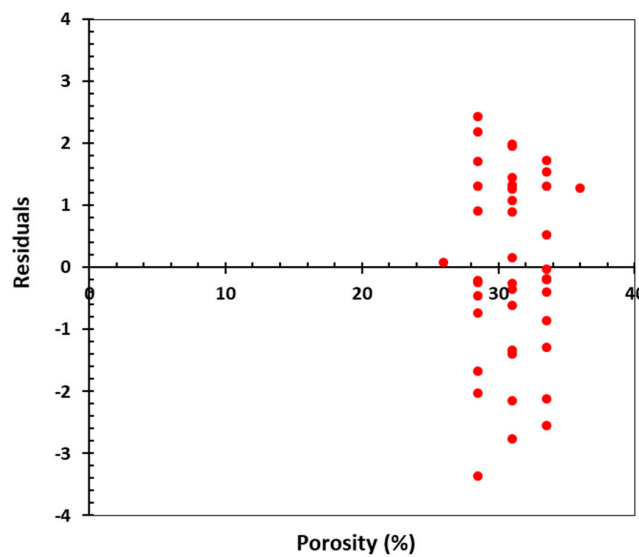


Figure 21. Residuals vs. porosity for the database analyzed.

Table 3 presents the values for the correlation coefficients, standard errors, and the ranges for the coefficients involved in the equation for the CSOR. Needless to mention that definitions of all parameters introduced in Tables 3–5 are presented in Section 4 of this paper. Since the variables such as  $K_m$  (mD),  $K_f$  (mD),  $(\varphi)$  porosity (%),  $S_o$  (%) have high magnitudes, their coefficients must be 4 to 6 digits significant while using regression correlations.

Table 5. ANOVA table for CSOR regression analysis.

Source	DF	SS	MS	F
Regression	14	2598.98	185.64	128.76
Residual	15	21.63	1.44	-
Total	29	2620.61	-	-

Recovery Factor (RF) is also an important asset assessment parameter, and a reliable tool to predict RF, even if only in a statistical manner, it would be valuable for first-order screening. Estimation of production performance is possible with initial and residual oil saturation data. The irreducible oil saturation is normally not known until the end of the thermal operation. Nevertheless, a correlation was established for RF prediction in terms of formation, steam, and oil properties considering the production history of some field pilots and laboratory tests data. To derive the following equation, a similar method as that for CSOR was implemented using statistical regression analysis:

$$\begin{aligned}
 RF = & a_{15} + a_{16}S_o + a_{17}h + a_{18}q_s + a_{19}\varphi_e + a_{20}K_m + a_{21}x_s + a_{22}\mu_o + a_{23}\frac{K_m h}{\mu_o} + \\
 & a_{24}S_o\varphi_e + a_{25}q_s x_s + a_{26}\frac{S_o\varphi_e h K_m q_s}{\mu_o x_s} + a_{27}q_s\varphi_e + a_{28}\frac{K_f}{K_m}
 \end{aligned} \quad (16)$$

The product of fracture permeability and matrix permeability and the interaction of all contributing parameters affect the RF in the form of “combinatory effects”. Table 4 contains data on the statistical correlation coefficients.

The corresponding ANOVA for CSOR is presented in Table 5. The  $F$  observed for CSOR (196.645) exceeds the critical value (2.31). Hence, all of the parameters considered in multivariable linear regression analysis of CSOR and their attributed effects are significant and cannot be ignored to simplify the statistical model.

There is a vigorous dependence between the objective function (RF) and the process variables implemented in the statistical analysis. This is evident considering the high values of the observed “ $F$ ”

compared with the tabulated critical value (Table 6). It is also evident from Table 6 that the regression analysis for RF has an acceptable accuracy.

**Table 6.** ANOVA Table for RF during steamflooding.

Source	DF	SS	MS	F
Regression	13	657.68	50.59	70.60
Residual	27	19.34	0.72	-
Total	40	677.03	-	-

The magnitudes of the squared residuals (Table 7) can be used to check the accuracy of a linear regression. The results obtained in this research suggest a reasonable compatibility between the measured (field pilots and experimental data) and the forecasts (regression analysis). The proposed model and the associated curves can be implemented to forecast CSOR and RF in any given VO NFRs given the limitations of the database.

**Table 7.** Summary of the Statistical Linear Regressions.

Objective Function	Multiple R	$R^2$	Standard Error	Number of Observations
CSOR	0.97	0.96	0.01	30
RF	0.98	0.96	0.08	41

Based on this study, the in situ oil viscosity and the initial oil saturation are the most significant factors influencing CSOR and RF. This was expected because of the nature of the steam processes.

According to the statistical information provided in Tables 7 and 8, there is an admissible match between the predicted and measured RF and CSOR. As shown in Table 8, the statistical parameters (e.g.,  $R^2$ , minimum percentage error (MIPE), maximum percentage error (MAPE), and mean squared error (MSE)) for the new models obtained in this study and the relationships developed by other researchers such as Chu [20], Vogel [75], Boberg [66], and Butler [67] were obtained and compared. The statistical models developed, presented, and examined in this paper are more accurate in estimation of RF and CSOR as they appreciate from higher  $R^2$  and lower MIPE, MAPE, and MSE.

**Table 8.** Performances of previous predictive models and statistical correlations obtained in the current study.

Statistical Parameter	Chu [20]		Vogel [75]		Boberg [66]		Butler [67]		New Models	
	RF	CSOR	RF	CSOR	RF	CSOR	RF	CSOR	RF	CSOR
$R^2$	0.97	0.94	0.92	0.93	0.91	0.93	0.93	0.91	0.98	0.97
MSE	0.09	0.09	0.14	0.15	0.15	0.16	0.15	0.11	0.06	0.08
MIPE (%)	7.69	9.87	7.69	10.58	9.11	10.78	9.12	10.41	5.35	6
MAPE (%)	12.64	14.54	13.48	15.17	14.52	16	14.45	15.54	10.32	11.12

The viscosity of cases analyzed ranges from 6 to 936 cP, thus the reservoirs are heavy oil reservoirs except for one medium heavy and one light oil reservoir in a NFR. The reservoir depth for the studied cases varies from 134 to 1350 m. This range covers the lower and upper limits of applicability of steamflooding. Matrix porosity and permeability vary from 0.12 to 0.35 and 1–4 D. In addition, the fracture “permeability” is between 1 and 1,000 D. These ranges represent an acceptable coverage for variation in parameters expected in such heterogeneous reservoirs despite small number of field pilots of steamflooding in NFRs.

## 7.2. Screening of a Heavy Oil Field for Steamflooding

The Kuh-e-Mond heavy oil field, the largest on-shore heavy oil field in Iran, is a giant anticline located in the southwest of the country with a NW-SE trend. The field is 90 km long and 16 km



wide with an estimated minimum heavy oil resource base of  $10 \times 10^9$  b OOIP. The heavy oil is found in three separate layers with depths ranging from 400 to 1,200 m and oil viscosities of 550 to 1120 cP in situ [78–80]. The trap structure formed during the main phase of Zagros folding in the late Miocene and Pliocene, as shown by the relatively constant thickness of the lower Miocene succession [78–80]. According to petrophysical evaluations, the Jahrum Formation limestone is a poor reservoir; only part of it has good porosity ( $\phi$ ) in the range of 0.24 to 0.31 and water saturation ( $S_w$ ) around 0.20. This formation contains immobile heavy oil. The OOIP has been estimated at about  $3 \times 10^9$  b [78–80]. The Sarvak Formation, Cenomanian in geological age, is predominantly composed of intensely fractured marly limestone with some shale interbeds. The formation is divided into three main units in the study area: upper, middle, and lower units. The upper unit is composed of limestone with some weakly argillaceous impurities. Shale and marls are main rock types in the middle Sarvak. Finally, the lower Sarvak predominantly consists of marly limestone with shale. Considering the intensely fractured nature of the Sarvak formation, heavy mud losses were reported during the drilling. The heavy oil resource in the Sarvak reservoir (OOIP) is estimated at  $3.6 \times 10^9$  barrels [78].

Lithostratigraphic information and fluid properties for the heavy oil reservoirs at the study area were collected, assessed, and summarized as presented in Table 9. In assembling this database, data from various sources such as drilling logs, geophysical logs, and field and laboratory test data were used. The average magnitudes of reservoir and fluid properties were determined for each reservoir using the available data. Single values reported for some properties of the reservoirs here are the average values of the reservoirs' parameters; while, the properties may change with respect to the location within the field.

**Table 9.** Reservoir and fluid properties of reservoirs at the Kuh-e-Mond heavy oil field.

Reservoir Abbreviation	Jahrum	Sarvak
Lithology	Dolomite and Dolomitic Limestone	Limestone
Depth (m)	680–900	1100–1200
Thickness (z) (m)	320	100
Net to Gross Ratio (%)	31	47
Net Pay Thickness (m)	99	47
Oil Viscosity (In situ) (cP)	1160	570
Temperature (T) (In situ) °F	70	110
Matrix Permeability (mD)	1	0.2–1.4
Fracture Permeability (mD)	300–500	350–500
Porosity ( $\phi$ ) (Fraction)	0.19	0.16
Oil Saturation (Fraction)	0.66	0.46

Based on the predictive regression models, if 200 to 250 b/d of steam with 80% to 90% quality is injected into the formation then CSOR and RF will be in the ranges of 6 to 7.2 and 41% to 49%, respectively, for the Jahrum HO reservoir. These ranges will be 6.3 to 8 and 37% to 44% for CSOR and RF in Sarvak HO reservoir. The screening results imply that Jahrum reservoir is technically recoverable by using steamflooding despite an average rock matrix porosity of 19%. This is mainly because of other commendatory factors such as depth, thick net pay, and relatively high oil saturation. The Sarvak reservoir met the technical screening criteria but the Jahrum reservoir is considered a moderately better candidate. Very low matrix permeability and low oil saturation (<50% PV) lead to lower RF and higher CSOR in the Sarvak reservoir. However, under current economic conditions, HO exploitation from these reservoirs remains economically unattractive.

We examined the developed correlations for estimation of CSOR and RF in oil sands and unconsolidated heavy oil sandstone reservoirs and compared the results with the CSOR estimations predicted by a correlation proposed by Chu [20]. The results suggest that the new correlations also can be used reliably to estimate CSOR and RF in oil sands and unconsolidated heavy oil sandstone reservoirs. The developed correlations can be considered a general form of correlations to be utilized

for wide ranges of reservoir properties from NFCRs to oil sands and unconsolidated heavy oil sandstone reservoirs.

During utilization of steam injection in any given heavy oil reservoir, laboratory experiments and field interposition can serve the operator to avoid or rectify high CSOR by selecting an appropriate production rate and/or steam injection rate. The recovery and injection rates affect thermodynamic conditions, steam/oil ratio, and composition of the liquid phase, which is mobilized and moving to the production well. Hence, utilizing experiments and statistical modeling (i.e., using different flow rates as various dynamic conditions) which is much inexpensive and yet faster compared with field trials will be definitely beneficial in systematic assessment of the performance of steamflooding in any given HO NFCR. Estimation of vital process performance indicators such as CSOR and RF can provide invaluable directions for optimum design of a recovery technology in terms of flow rate and thermodynamic status of the fluids. Furthermore, accurate prediction of RF and CSOR for a given HO NFCR can enable process engineers with reasonable rules of thumb to minimize heat loss, which can lead to notable steam condensation in the reservoir.

### 7.3. Limitations and Assumptions for the Correlations of CSOR and RF

Table 10 presents the range of variables contributed in the correlations developed to forecast of RF and CSOR in NFCRs.

**Table 10.** Range of variables to estimate RF and CSOR.

	Parameter	Min	Max
<b>Input</b>	Depth (m)	134	1350
	Matrix porosity (Fraction)	0.12	0.35
	Matrix permeability (mD)	1	400
	Fracture permeability (D)	1	1000
	Oil viscosity (cP)	6	936
	Initial oil saturation (Fraction)	0.3	0.9
	Steam quality	0.3	1
<b>Output</b>	Recovery factor, RF, (Fraction)	0.4	0.7
	Cumulative steam oil ratio (CSOR)	3.0	10.0

We identified and acknowledged the following sets of limitations for the proposed statistical models. However, in practice they remain as appropriate and accurate predictive tools:

- (1) Porous medium is non-deformable (constant porosity assumption).
- (2) For mass, there is no source term except for the steam.
- (3) A majority of the experimental data used in this research study have been obtained from the experiments in two-dimensional (2-D) porous systems.
- (4) The correlations are only valid in the range of parameters used in the current study. Ranges of fluid and porous media properties in oil fields are almost the same as in the experimental studies considered in this statistical investigation.
- (5) The Darcy law is valid throughout the EOR process. Flow in porous media is mostly laminar (i.e.,  $Re < 1$ ) during steamflooding.
- (6) RF and CSOR forecasts are not affected greatly by the geometry of the physical models (experimental data taken from the literature) used in the experimental works (taken from the literature). It only influences the residual oil saturation, moderately. This is because the geometry dominates the shape of the corners and the end points in a porous system. In addition, in these experiments no changes was observed for a high capillary threshold and permeability with regard to geometry variations in the porous system.
- (7) There were a certain number of porous media with specific fracture patterns selected for this statistical study. The proposed statistical models are very accurate for these fracture

configurations. Thus, the only major limitation here is the type of fracture configuration. Nevertheless, if the effective fracture permeability is known for a porous system with unknown fracture configuration then the developed statistical models can be used to forecast the RF and CSOR with an acceptable accuracy.

Steamflooding and its variants utilizing either vertical, inclined, or horizontal wells can be used for any type of reservoirs regardless of the reservoir rock type if the oil viscosity is less than 5000 cP. This also includes conventional reservoirs containing light oil. In this case, steam and the resultant heat in the reservoir serve as stimulant rather than sweeping the oil or lowering down the oil viscosity (the well-known piston model). The only exception would be highly porous rocks such as diatomite and chalk which are also structurally very weak when exposed to heat [81,82]. In addition, the correlations introduced in this paper can be used to assess the performance of steamflooding in non-fractured reservoirs, as well. In fact, both fractured and non-fractured media are considered in the correlations and in the case of non-fractured media where there is no natural fractures, those parameters will be cancelled from the equations and the remaining terms can be used to evaluate the performance of the process in non-fractured systems (single porosity systems). The proposed correlations can be used as a proxy to assess the feasibility of the process in the candidate reservoirs. However, CSOR is a strong indicator of economic feasibility of any thermal operations under the current economic climate. For example, in Canada any thermal operations with CSORs below 3 are considered economic. Considering decades of experience in thermal operations in Canada especially for well-known and commercialised technologies such as SAGD and HCS, wealth of available field data, and advanced process optimization practices, the CSOR is now down to less than 2. Considering the case study presented here, this heavy oil field is a poor candidate for steamflooding. However, utilizing long horizontal wells will increase the oil recovery and will reduce the CSOR in the case studied. In addition, adopting cyclic steam stimulation processes can reduce the steam requirements, lower down the CSOR, and increase the RF and oil production rate. Nevertheless, the correlations developed and presented here can only be used for estimation of RF and CSOR in thermal heavy oil operations utilizing vertical wells. Clearly, new sets of correlations or models will be needed to predict performance of steam processes utilizing horizontal wells. Such projects still do not exist (therefore no field data is available at the moment) when it comes to carbonate reservoirs. Some steam injection variants such as HCS process are being tried in bitumen saturated Devonian carbonates in Alberta, Canada.

## 8. Conclusions

This article presents new statistical models to forecast cumulative steam to oil ratio (CSOR) and recovery factor (RF) in naturally fractured reservoirs under steamflooding. The CSOR and RF were statistically correlated in terms of physical properties of the oil, reservoir fluid and rock properties, and steam properties. The following conclusions seem reasonable, despite a modest database:

- (1) The correlations developed in this study are derived from data obtained from field and laboratory tests. High correlation coefficients ( $R^2$ ) show that the multivariable regression method used is a strong predictor of the economic assessment factors CSOR and RF.
- (2) The errors involved in even the worst cases were less than 10%, giving confidence that first-order economic decisions can be made with these relationships.
- (3) The parameters considered for regression analysis are not able to forecast the oil production characteristics of steamflooding in NFCRs if they are used alone. Combination terms for the main variables were used that led to the reliable outcome.
- (4) Initial oil saturation and oil viscosity have the greatest impact on predictor models for CSOR and RF. Nevertheless, all of the chosen parameters have a significant influence on the predictions; therefore, none of them should be abandoned in the search for a simpler model.

- (5) Comparison of statistical correlations developed in this paper, and the previous correlations shows that the newly defined equations can predict steamflooding efficiency in heavy oil NFCRs with high accuracy such that the maximum error percentage is lower than 12% for the equations obtained in this study.
- (6) The proposed correlations were applied to predict CSOR and RF in two fractured heavy oil reservoirs, with apparently good results. This supports the use of these relationships for initial technical feasibility assessment of VO NFCRs for vertical well steamflooding.

**Acknowledgments:** The authors would like to thank the editor and the assistant editor (Jennie Hu) of the journal *Energies* for handling this manuscript. We also wish to thank Mirosław (Mirek) Slowakiewicz and two other anonymous reviewers for their critical review of the manuscript and providing us with their valued comments and fair criticism, which helped us to improve the overall quality of the manuscript.

**Author Contributions:** Ali Shafiei conceived the idea, collected the data, and wrote the first draft of the manuscript. Mohammad Ali Ahmadi, Maurice B. Dusseault, Ali Elkamel, Sohrab Zendehboudi, and Ioannis Chatzis have contributed to the manuscript during the model development stage, the discussion of results, and during the writing stage.

**Conflicts of Interest:** The authors declare no conflict of interest.

## Nomenclature

### Acronyms or Abbreviations

ANOVA	Analysis of Variance
CSOR	Cumulative Steam to Oil Ratio
CSS	Cyclic Steam Stimulation
EIA	the U.S. Energy Information Administration
HO	Heavy Oil
MCWEB	1000 Cold Water Equivalent Barrels
NFCRs	Naturally Fractured Carbonates Reservoirs
NFR	Naturally Fractured Reservoir
OSR	Oil Steam Ratio
RF	Recovery Factor
SD	Steam Drive
SF	Steamflooding
USGS	the United States Geological Survey
VO NFCRs	Viscous Oil Naturally Fractured Carbonates Reservoirs
VO	Viscous Oil
XHO	Extra Heavy Oil

### Symbols: Latin, Then Greek

$\bar{y}$	Average of all data points of dependent variable in Equation (13)
$\hat{y}_i$	Predicted data in Equation (13)
$\varphi$	Total effective porosity
$\dot{A}$	rate of change in the planar area of the steam chamber, (m <sup>2</sup> /t)
$\mu$	Dynamic viscosity (kg·m/s or cP)
$A$	Planar area of the steam chamber, (m <sup>2</sup> )
$b$	Exponent in Cardwell and Parson's equation for relative permeability (dimensionless)
$C_{vo}$	Overburden volumetric heat capacity, (MJ/m <sup>3</sup> ·K)
$C_{vr}$	Initial reservoir volumetric heat capacity, (MJ/m <sup>3</sup> ·K)
$D$	Reservoir depth, (m)
$e$	Error value in Equations (7), (8) and (12)
$g$	Gravity acceleration, (m/year <sup>2</sup> )
$H$	Enthalpy, (MJ/m <sup>3</sup> )
$h$	Height of reservoir above producer, (m)
$H_{lv}$	Latent heat of condensation of steam, (MJ/m <sup>3</sup> )
$H_s$	Height of the steam chamber, (m)

$k$	Number of regressor variables
$K$	Permeability, (m <sup>2</sup> )
$K_f$	Intrinsic permeability of the fracture, (Darcy or m <sup>2</sup> )
$K_m$	Permeability of matrix in the model, (Darcy or m <sup>2</sup> )
$K_t$	Overburden thermal conductivity, (MJ/m·K·year)
$n$	Number of observations or data points in Equation (13)
PV	Pore volume, (m <sup>3</sup> )
$q_s$	Steam injection rate, (bbl/d)
RF	Recovery Factor
$S$	Liquid saturation
$T$	Temperature, (°C)
$t$	Time since first steam injection, (year)
$V_{sz}$	Volume of the steam chamber, (m <sup>3</sup> )
$x_i$	Regression variables in Equations (7) to (12)
$x_s$	Steam quality
$y$	System response in Equations (7), (9), (10) and (12)
$y_i$	Real or observed data in Equation (13)
$\beta$	Effective sweep efficiency factor, dimensionless
$\beta_i$	Regression coefficients in Equations (5) to (7)
$\Delta$	Difference operator
$\Delta S_o$	Initial minus residual oil saturation, dimensionless
$\Delta T$	Temperature rise above initial condition, (°C)
$\eta_s$	Effective sweep efficiency, dimensionless
$\nu_s$	Kinematic viscosity of the oil at the temperature of the steam, (m <sup>2</sup> /year)
$\rho$	Density of fluid, (kg/m <sup>3</sup> )
<i>Subscripts</i>	
$f$	fracture
$i$	number of test runs
$m$	matrix
max	maximum
min	minimum
<i>Metric Conversion Factors</i>	
°F	(°C × 1.8) + 32
1 barrel oil	0.159 m <sup>3</sup>
1 psi	6.8947 kPa
1 psi/ft	22.62 kPa/m or 22.62 MPa/km

## References

1. U.S. Energy Information Administration (EIA). International Energy Outlook 2017. Available online: [https://www.eia.gov/outlooks/ieo/pdf/0484\(2017\).pdf](https://www.eia.gov/outlooks/ieo/pdf/0484(2017).pdf) (accessed on 6 December 2017).
2. International Energy Agency (IEA). World Energy Outlook 2015. Available online: <http://www.iea.org/publications/freepublications/publication/WEO2015.pdf> (accessed on 6 December 2017).
3. International Energy Agency (IEA). International Energy Outlook 2011, EIA-DOE-0484 (2012). Available online: [https://www.iea.org/publications/freepublications/publication/WEO2011\\_WEB.pdf](https://www.iea.org/publications/freepublications/publication/WEO2011_WEB.pdf) (accessed on 6 December 2017).
4. Höök, M.; Hirsch, R.; Aleklett, K. Giant Oil Field Decline Rates and Their Influence on World Oil Production. *Energy Policy* **2009**, *37*, 2262–2272. [CrossRef]
5. Dusseault, M.B.; Shafiei, A. Oil Sands. In *Ullmann's Encyclopedia of Chemical Engineering*; Wiley: Hoboken, NJ, USA, 2011; 52p.
6. Shafiei, A. Mathematical and Statistical Investigation of Vertical Well Steamflooding in Viscous Oil Naturally Fractured Carbonate Reservoirs. Ph.D. Thesis, University of Waterloo, Waterloo, ON, Canada, 2013.

7. Briggs, P.J.; Baron, R.P.; Fulleylove, R.J.; Wright, M.S. Development of heavy oil reservoirs. *J. Pet. Technol.* **1988**, *40*, 206–214. [[CrossRef](#)]
8. Bağcı, A.S.; Shafiei, A.; Dusseault, M.B. Case Histories for Heavy Oil Recovery in Naturally Fractured Carbonate Reservoirs in the Middle East. In Proceedings of the 2nd World Heavy Oil Congress, Edmonton, AB, Canada, 10–12 March 2008.
9. Davidson, L.B.; Miller, F.G.; Mueller, T.D. A Mathematical Model of Reservoir Response during the Cyclic Injection of Steam. *SPE J.* **1967**, *7*, 174–188. [[CrossRef](#)]
10. Shafiei, A.; Dusseault, M.B.; Zendehboudi, S.; Chatzis, I. A New Screening Tool for Evaluation of Steamflooding Performance in Naturally Fractured Carbonate Reservoirs. *Fuel* **2013**, *108*, 502–514. [[CrossRef](#)]
11. Coats, K.H.; George, W.D.; Chu, C.; Marcum, B.E. Three-Dimensional Simulation of Steamflooding. *SPE J.* **1974**, *14*, 573–592. [[CrossRef](#)]
12. Chu, C.; Trimble, A.E. Numerical Simulation of Steam Displacement Field Performance Applications. *J. Pet. Technol.* **1975**, *27*, 765–776. [[CrossRef](#)]
13. Neuman, C.H. A Mathematical Model of the Steam Drive Process Applications. In Proceedings of the SPE Improved Oil Recovery Symposium, Tulsa, OK, USA, 22–24 April 1974. Paper # 4757-MS.
14. Myhill, N.A.; Stegemeier, G.L. Steam Drive Correlation and Prediction. *J. Pet. Technol.* **1978**, 173–182. [[CrossRef](#)]
15. Farouq Ali, S.M. Steam injection theory—A unified approach. In Proceedings of the California Regional Meeting of the Society of Petroleum Engineers, San Francisco, CA, USA, 24–26 March 1982; SPE # 10746.
16. Gomaa, E.E. Correlations for Predicting Oil Recovery by Steamflood. *J. Pet. Technol.* **1980**, *32*, 325–332. [[CrossRef](#)]
17. Yortsos, Y.C.; Gavalas, G.R. Analytical Modeling of Oil Recovery by Steam Injection: Part I—Upper Bounds. *SPE J.* **1981**, *21*, 162–178. [[CrossRef](#)]
18. Yortsos, Y.C.; Gavalas, G.R. Analytical Modeling of Oil Recovery by Steam Injection: Part 2—Asymptotic and Approximate Solutions. *SPE J.* **1981**, *21*, 179–190. [[CrossRef](#)]
19. Neuman, C.H. A Gravity Override Model of Steamdrive. *J. Pet. Technol.* **1985**, 163–169. [[CrossRef](#)]
20. Chu, C.F. Prediction of steamflood performance in heavy oil reservoirs using correlations developed by factorial design method. In Proceedings of the South California Regional Meeting, Ventura, CA, USA, 4–6 April 1990; SPE # 20020.
21. Torabzadeh, S.J.; Kumar, M.; Hoang, V.T. Performance Correlations for Steamflood Field Projects. In Proceedings of the SPE California Regional Meeting, Ventura, CA, USA, 4–6 April 1990; SPE # 20036.
22. Jensen, T.B.; Sharma, M.P.; Harris, H.G. An improved evaluation model for steam-drive projects. *J. Pet. Sci. Eng.* **1991**, *5*, 309–322. [[CrossRef](#)]
23. Gajdica, R.J.; Brigham, W.E.; Aziz, K. A Semi-analytical Thermal Model for Linear Steamdrive. *SPE Res. Eng.* **1993**, 73–79. [[CrossRef](#)]
24. Jones, J. Predicting performance of steam floods with analytical models. *J. Pet. Sci. Eng.* **1993**, *9*, 9–15. [[CrossRef](#)]
25. Donaldson, A.B.; Donaldson, J.E. Dimensional Analysis of the Criteria for Steam Injection. In Proceedings of the 1997 SPE Western Regional Meeting, Long Beach, CA, USA, 25–27 June 1997; SPE # 38303.
26. Edmunds, N.; Peterson, J. A Unified Model for Prediction of CSOR in Steam-Based Bitumen Recovery. In Proceedings of the Petroleum Society's 8th Canadian International Petroleum Conference, Calgary, AB, Canada, 12–14 June 2007.
27. Miura, K.; Wang, J. An Analytical Model to Predict Cumulative Steam Oil Ratio (CSOR) in Thermal Recovery SAGD Process. In Proceedings of the Canadian Unconventional Resources and International Petroleum Conference, Calgary, AB, Canada, 19–21 October 2010.
28. Sahuquet, B.C.; Ferrier, J.J. Steam-Drive Pilot in a Fractured Carbonated Reservoir: Lacq Supérieur Field. *J. Pet. Technol.* **1982**, *34*, 873–880. [[CrossRef](#)]
29. Sahuquet, B.C.; Spreux, A.M.; Corre, B.; Guittard, M.P. Steam Injection in a Low Permeability Reservoir through a Horizontal Well in Lacq Supérieur Field. In Proceedings of the SPE Annual Technical Conference and Exhibition, New Orleans, LA, USA, 23–26 September 1990; SPE # 20526.
30. Chierici, A.; Delle Canne, D.; Properzi, O. Steam Drive in a Fractured Carbonate: The Vallecupa, Italy, Pilot Plant. In Proceedings of the Third European Meeting on Improved Oil Recovery, Rome, Italy, 16–18 April 1985.



31. Nakamura, S.; Sarma, H.K.; Umucu, T.; Issever, K.; Kanemitsu, M.A. Critical Evaluation of a Steamflood Pilot in a Deep Heavy Carbonate Reservoir in Ikiztepe Field, Turkey. In Proceedings of the SPE Annual Technical Conference and Exhibition, Dallas, TX, USA, 22–25 October 1995; SPE # 30727.
32. Ono, K. Successful field pilots in a carbonate heavy oil reservoir in the Ikiztepe Field, Turkey. *J. Jpn. Assoc. Pet. Technol.* **1997**, *62*, 103–111. [[CrossRef](#)]
33. Snell, J.S.; Close, A.D. Yates Field Steam Pilot Applies Latest Seismic and Logging Monitoring Techniques. In Proceedings of the 1999 SPE Annual Technical Conference and Exhibition, Houston, TX, USA, 3–6 October 1999; SPE # 56791.
34. Snell, J.S.; Wadleigh, E.E.; Tilden, J. Fracture Characterization a Key Factor in Yates Steam Pilot Design and Implementation. In Proceedings of the 2000 SPE International Petroleum Conference and Exhibition in Mexico, Villahermosa, Mexico, 1–3 February 2000; SPE # 59060.
35. Dehghani, K.; Ehrlich, R. Evaluation of the Steam-Injection Process in Light-Oil Reservoirs. *SPE Res. Eval. Eng.* **2001**, *4*, 395–405. [[CrossRef](#)]
36. Barge, D.; Al-Yami, F.; Uphold, D.; Zahedi, A.; Deemer, A.; Carreras, P.E. Steamflood Piloting the Wafra Field Eocene Reservoir in the Partitioned Neutral Zone, Between Saudi Arabia and Kuwait. In Proceedings of the SPE Middle East Oil and Gas Show and Conference, Manama, Bahrain, 15–18 March 2009; SPE # 120205.
37. Brown, J.; Deemer, A.; Al-Dhafeeri, F.; Lekia, S.; Hoadley, S.; Al-Mutairi, G.; Al-Yami, F.; Barge, D. Early Results from a Carbonate Steamflood Pilot in 1st Eocene Reservoir, Wafra Field, PZ. In Proceedings of the SPE Heavy Oil Conference and Exhibition, Kuwait City, Kuwait, 12–14 December 2011; SPE # 150605.
38. Hoadley, S.; Al-Yami, F.; Deemer, A.; Brown, J.; Al-Mutairi, G.; Lekia, S.; Al-Dhafeeri, F.; Al-Odhailah, F.; Barge, D. Surveillance Improvements during the Implementation of a Large Scale Carbonate Steamflood Pilot, Wafra field, PZ. In Proceedings of the SPE Heavy Oil Conference and Exhibition, Kuwait City, Kuwait, 12–14 December 2011; SPE # 150608.
39. Meddaugh, W.S.; Osterloh, W.T.; Toomey, N.; Bachtel, S.; Champenoy, N.; Rowan, D.; Gonzalez, G.; Aziz, S.; Hoadley, S.F.; Brown, J.; et al. Impact of Reservoir Heterogeneity on Steamflooding, Wafra First Eocene Reservoir, Partitioned Zone (PZ), Saudi Arabia and Kuwait. In Proceedings of the SPE Heavy Oil Conference and Exhibition, Kuwait City, Kuwait, 12–14 December 2011; SPE # 150606.
40. Osterloh, W.T.; Mims, D.S.; Meddaugh, W.S. Probabilistic Forecasting and Model Validation for the 1st Eocene Large Scale Pilot (LSP) Steamflood, Partitioned Zone (PZ), Saudi Arabia and Kuwait. In Proceedings of the SPE Heavy Oil Conference and Exhibition, Kuwait City, Kuwait, 12–14 December 2011; SPE # 150580.
41. Gross, S.J.; Johansen, S.J.; Perinot, T.; Deemer, A.R.; Hoadley, S.F.; Meddaugh, W.S. Steamflood Pilot Design for the Wafra Field 2nd Eocene Reservoir in the Partitioned Zone (PZ), Saudi Arabia and Kuwait. In Proceedings of the SPE Heavy Oil Conference and Exhibition, Kuwait City, Kuwait, 12–14 December 2011; SPE # 150610.
42. Olsen, D.K.; Sarathi, P.S.; Schulte, R.K.; Giangiacomo, L.A. Case History of Steam Injection Operations at Naval Petroleum Reserve No. 3, Teapot Dome Field, Wyoming: A Shallow Heterogeneous Light-Oil Reservoir. In Proceedings of the International Thermal Operations Symposium, Bakersfield, CA, USA, 8–10 February 1993; SPE # 25786.
43. Couderc, B.M.; Verpeaux, J.F.; Monfrin, D.; Guettler, L.H. Emeraude Vapeur: A Steam Pilot in an Offshore Environment. *SPE Res. Eng.* **1990**, *5*, 508–516. [[CrossRef](#)]
44. Chu, C. State-of-the-Art Review of Steamflood Field Projects. *J. Pet. Technol.* **1985**, *37*, 1887–1902. [[CrossRef](#)]
45. Mollaei, A.; Maini, B.; Jalilavi, M. Investigation of Steam Flooding in Naturally Fractured Reservoirs. In Proceedings of the International Petroleum Technology Conference, Dubai, UAE, 4–6 December 2007.
46. Mollaei, A.; Maini, B. Steam Flooding of Naturally Fractured Reservoirs: Basic Concepts, Recovery Mechanisms, Process Improvements, Mechanism and Optimization of in situ CO<sub>2</sub> Generation. In Proceedings of the Petroleum Society's 8th Canadian International Petroleum Conference (58th Annual Technical Meeting), Calgary, AB, Canada, 12–14 June 2007. PETSOC-2007-128.
47. Van Heel, A.P.G.; van Dorp, J.J.; Boerrigter, P.M. Heavy-Oil Recovery by Steam Injection in Fractured Reservoirs. In Proceedings of the 2008 SPE/DOE Improved Oil Recovery Symposium, Tulsa, OK, USA, 19–23 April 2008; SPE # 113461.
48. Ashrafi, M.; Souraki, Y.; Karimaie, H.; Torsaeter, O. Experimental and Numerical Study of Steam Flooding in Fractured Porous Media. In Proceedings of the SPE Western North American Regional Meeting, Anchorage, AK, USA, 7–11 May 2011; SPE # 144462.

49. Souraki, Y.; Ashrafi, M.; Karimaie, H.; Torsæter, O. Experimental Investigation and Numerical Simulation of Steam Flooding in Heavy Oil Fractured Reservoir. In Proceedings of the SPE Western North American Region Meeting, Anchorage, AK, USA, 7–11 May 2011; SPE # 144552.
50. United States Congress Office of Technology Assessment. *Enhanced Oil Recovery Potential in the United States*; United States Congress Office of Technology Assessment: Washington, DC, USA, 1978; p. 234.
51. Yortsos, Y.C. *Visualization and Simulation of Immiscible Displacement in Fractured Systems Using Micromodels: Steam Injection*; DOE/BC/14899-25; University of Southern California: Los Angeles, CA, USA, 1995.
52. Tang, G.-Q.; Inouye, A.; Lowry, D.; Lee, V. Recovery Mechanism of Steam Injection in Carbonate Reservoir. In Proceedings of the SPE Western North American Regional Meeting, Anchorage, AK, USA, 7–11 May 2011; SPE # 144524.
53. Taber, J.J.; Martin, F.D.; Seright, R.S. EOR screening criteria revisited—Part 1: Introduction to screening criteria and enhanced recovery field projects. *SPE Res. Eng.* **1997**, *12*, 189–198. [[CrossRef](#)]
54. Worldwide EOR Survey. *OGJ* **1996**, *94*, 45–61.
55. Worldwide EOR Survey. *OGJ* **1998**, *96*, 59–74.
56. Worldwide EOR Survey. *OGJ* **2004**, *102*, 53–65.
57. Worldwide EOR Survey. *OGJ* **2006**, *104*, 45–57.
58. Worldwide EOR Survey. *OGJ* **2008**, *106*, 47–59.
59. Special Report: EOR/Heavy Oil Survey: 2010 worldwide EOR survey. *OGJ* **2010**, *108*.
60. Special Report: EOR/Heavy Oil Survey: CO<sub>2</sub> miscible and steam dominate enhanced oil recovery processes. 2010. *OGJ* **2010**, *108*.
61. De Haan, H.J.; Van Lookeren, J.A. Early results of the first large-scale steam soak project in the Tia Juana Field, Western Venezuela. *J. Pet. Technol.* **1969**, *21*, 101–110. [[CrossRef](#)]
62. Bursell, C.G.; Pittman, G.M. Performance of Steam Displacement in the Kern River Field. *J. Pet. Technol.* **1975**, *27*, 997–1004. [[CrossRef](#)]
63. Oglesby, K.D.; Blevins, T.R.; Rogers, E.E.; Johnson, W.M. Status of the 10-Pattern Steamflood, Kern River Field, California. *J. Pet. Technol.* **1982**, *34*, 2251–2257. [[CrossRef](#)]
64. Farouq Ali, S.M. Current status of steam injection as a heavy oil recovery method. *J. Can. Pet. Technol.* **1974**, *13*, 54–68. [[CrossRef](#)]
65. Farouq Ali, S.M.; Meldau, R.F. Current steamflood technology. *J. Pet. Technol.* **1979**, *31*, 1332–1342. [[CrossRef](#)]
66. Boberg, T.C. *Thermal Methods of Oil Recovery*; Wiley: New York, NY, USA, 1988; ISBN 0471633003, 9780471633006.
67. Butler, R.M. *Thermal Recovery of Oil and Bitumen*; Prentice Hall: Upper Saddle River, NJ, USA, 1991.
68. Dusseault, M.B. Screening criteria and technology sequencing for in-situ viscous oil production. In *Heavy-Oil and Oil-Sand Petroleum Systems in Alberta and Beyond: AAPG Studies in Geology 64*; Hein, F.J., Leckie, D., Larter, S., Suter, J.R., Eds.; AAPG: Tulsa, OK, USA; Canadian Heavy Oil Association: Calgary, AB, Canada; AAPG Energy Minerals Division: Tulsa, OK, USA, 2013; pp. 655–668. [[CrossRef](#)]
69. Hernandez, J.A.M.; Trevisan, O.V. Heavy oil recovery mechanisms during steam injection in naturally fractured reservoirs. In Proceedings of the 2007 SPE Latin American and Caribbean Petroleum Engineering Conference, Buenos Aires, Argentina, 15–18 April 2007; SPE # 107372.
70. Briggs, P.J. A Simulator for the Recovery of Heavy Oil from Naturally Fractured Reservoirs Using Cyclic Steam Injection. In Proceedings of the Middle East Oil Show, Manama, Bahrain, 11–14 March 1989; SPE # 17954.
71. Reis, J.C. Oil Recovery Mechanisms in Fractured Reservoirs during Steam Injection. In Proceedings of the 1990 SPE/DOE Seventh Symposium on Enhanced Oil Recovery, Tulsa, OK, USA, 22–25 April 1990; SPE # 20204.
72. Briggs, P.J.; Beck, D.L.; Black, C.J.J.; Bissell, R. Heavy oil from fractured carbonate reservoirs. *J. SPE Res. Eng.* **1992**, *7*, 173–179. [[CrossRef](#)]
73. Prats, M. Reservoir Mechanisms in Heavy Oil Production. In Proceedings of the 15th World Petroleum Congress, Beijing, China, 12–17 October 1997.
74. Mollaei, A.; Maini, B. Steam Flooding of Naturally Fractured Reservoirs: Basic Concepts and Recovery Mechanisms. *J. Can. Pet. Technol.* **2010**, *49*, 65–70. [[CrossRef](#)]
75. Vogel, J.V. Simplified Heat Calculations for Steamfloods. *J. Pet. Technol.* **1984**, 1127–1136. [[CrossRef](#)]
76. Montgomery, D.C. *Introduction to Statistical Quality Control*; John Wiley & Sons: New York, NY, USA, 2008.

77. Montgomery, D.C.; Runger, G.C. *Applied Statistics and Probability for Engineers, Student Solutions Manual*; John Wiley & Sons: New York, NY, USA, 2006.
78. Bashari, A. Occurrence of heavy crude oil in the Persian Gulf. In Proceedings of the 4th UNITAR/UNDP International Conference on Heavy Crude and Tar Sands, Edmonton, AB, Canada, 7–12 August 1988; pp. 203–214.
79. Moshtaghian, A.; Malekzadeh, R.; Azarpanah, A. Heavy oil discovery in Iran. In Proceedings of the 4th UNITAR/UNDP International Conference on Heavy Crude and Tar Sands, Edmonton, AB, Canada, 7–12 August 1988; pp. 235–243.
80. Kamali, M.R.; Rezaee, M.R. Burial history reconstruction and thermal modeling at Kuh-e-Mond, SW Iran. *J. Pet. Geol.* **2003**, *26*, 451–464. [[CrossRef](#)]
81. Shafiei, A.; Dusseault, M.B. Geomechanics of Thermal Oil Production from Carbonate Reservoirs. *J. Porous Media* **2014**, *17*, 301–321. [[CrossRef](#)]
82. Shafiei, A.; Dusseault, M.B. Geomechanics of Thermal Viscous Oil Production in Sandstones. *J. Pet. Sci. Eng.* **2013**, *103*, 121–139. [[CrossRef](#)]



© 2018 by the authors. Licensee MDPI, Basel, Switzerland. This article is an open access article distributed under the terms and conditions of the Creative Commons Attribution (CC BY) license (<http://creativecommons.org/licenses/by/4.0/>).